

An Unexpected Journey in Rotorcraft CFD

Applied Modeling & Simulation Seminar

by

Neal M. Chaderjian

NASA Ames Research Center

Moffett Field, CA, USA

February 24, 2015





Background

- Rotorcraft Aeromechanics: The interaction between rotor aerodynamics and structures
 - ❖ Rotor blades can encounter tip vortices from other blades
 - Blade vortex interaction (BVI) affects performance, noise and vibration
 - ❖ Helicopter blades are highly flexible (UH-60 rotor tip moves 3 ft vertically)
 - ❖ Trimmed blade motions for steady flight
- Rotorcraft analysis is time dependent and multidisciplinary (CFD, CSD, Trim)

Bell Boeing V22 Osprey **Tiltrotor**



Sikorsky UH-60 Blackhawk **Helicopter**



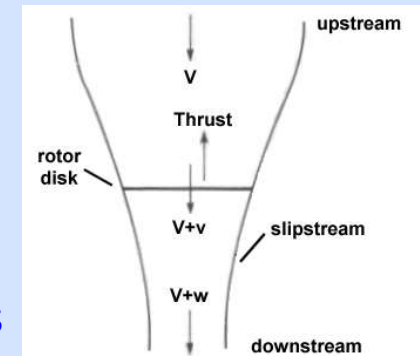


Motivation

- Figure of merit (FM) and rotor wakes simulations were inaccurate
 - ❖ FM is a measure of rotor blade efficiency
 - 2.4% average error (2007 NASA SOA report)
 - CFD typically under predicts FM by 2-6%
 - Every 0.5% error means one less passenger
- Recent studies indicate there is confusion about the relevant issues
 - ❖ Computational resources often limit grid resolution and run time
 - ❖ Turbulence models and poor wake-grid resolution greatly diffuse the rotor blade tip vortices
 - ❖ Concern for the effects of turbulent transition on the rotor blades
 - Inboard airfoils at typical flight Reynolds numbers
 - Micro air vehicles (MAV)
- Perception that most CFD codes give similar results
 - ❖ Physical and numerical issues not well understood
 - ❖ The practitioner makes a difference!

$$FM = \frac{C_{Q-ideal}}{C_{Q-actual}} = \frac{C_T^{3/2}}{\sqrt{2}C_Q}$$

Ideal Model

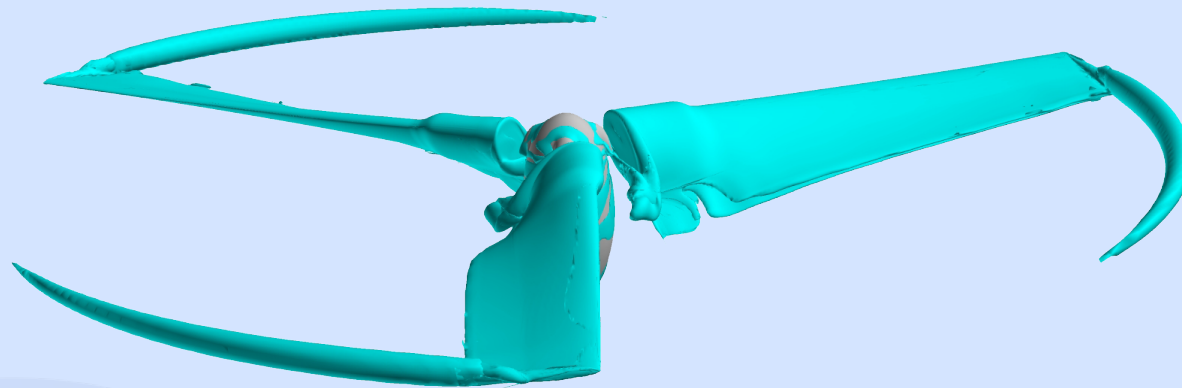




Motivation

- Does numerical diffusion of the vortex core significantly affect the FM?
- This question prompted research into adaptive mesh refinement (AMR)

Example of Highly Diffused CFD Vortices





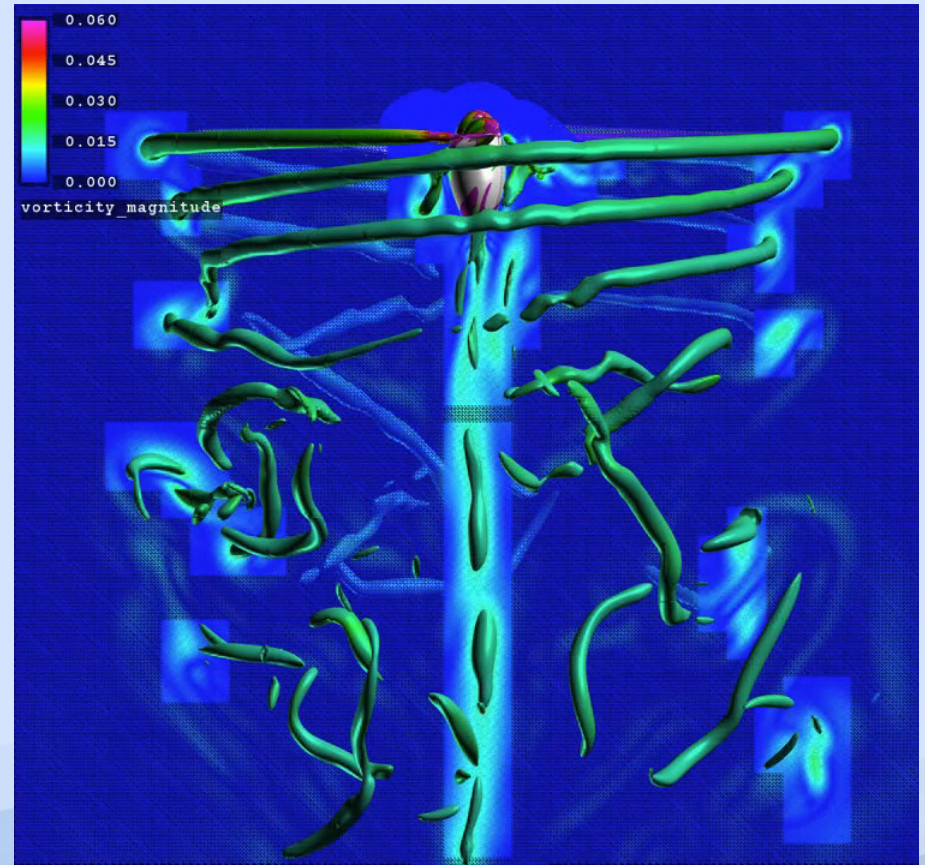
First OVERFLOW Attempt at Adaptive Mesh Refinement

TRAM Rotor: $M_{tip}=0.625$, $\theta=14^\circ$, $Re=2.1$ million

Spalart-Allmaras RANS model (SA-RANS)

AMR2: $\Delta=10\%$, 5% , $2.5\%c_{tip}$

- Begin with baseline wake ($\Delta=10\%c_{tip}$), and run AMR2 for 10 revolutions
 - ❖ But something unexpected happens!
 - ❖ This prompted a more careful study





NASA Rotary Wing (RW) Project Goal

*Improve prediction accuracy of with
physics-based tools such as
computational fluid dynamics (CFD)*

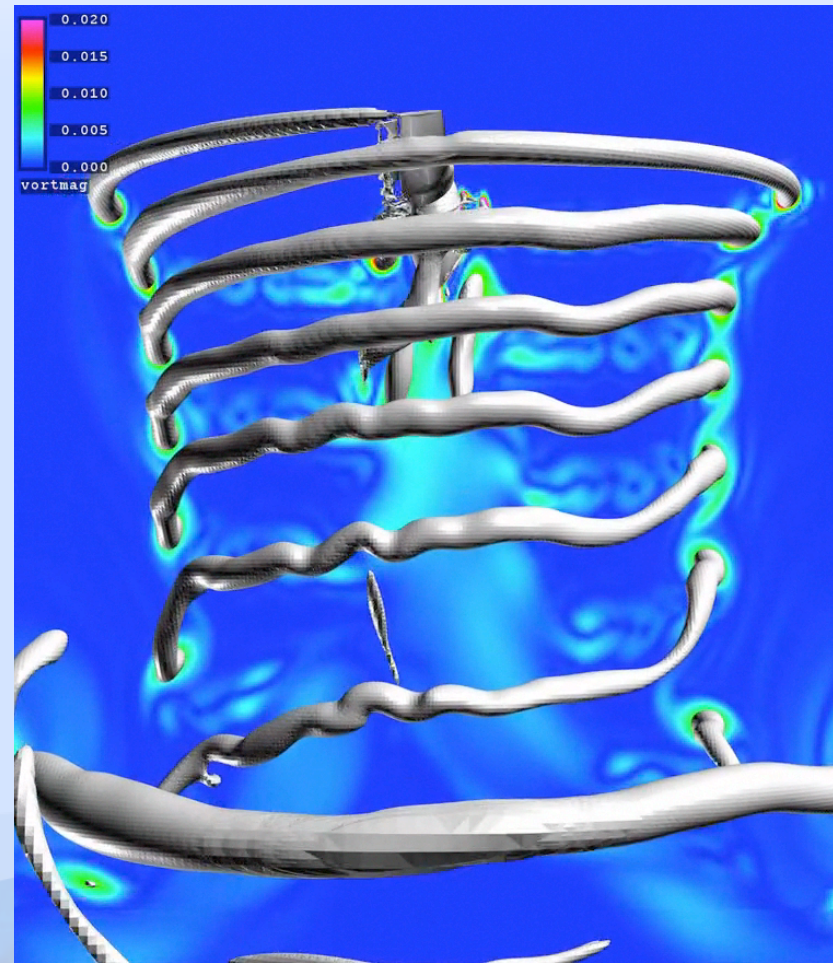
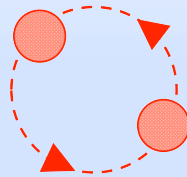
- Improve the prediction of FM with the Navier-Stokes equations
 - ❖ Better understanding of the physical and numerical processes
- Develop and demonstrate new capabilities within NASA's OVERFLOW CFD code
 - ❖ High-order spatial differences (from 3rd to 5th-order)
 - ❖ Adaptive mesh refinement (AMR) to better resolve rotor wakes
 - ❖ Turbulence model improvements



CFD State-of-the-Art (2010) V22 Osprey Rotor in Hover Begin from Impulsive Start

CFD Solution Process

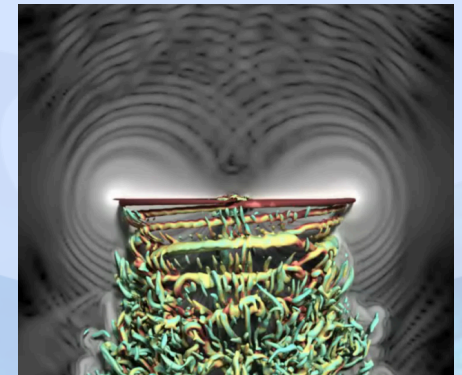
- Wake resolution: 10% C_{tip}
- Begin from impulsive start
- Vortex pairing ~ 7 revs
- Good FM statistics 20-30 revs
- Experiment averages FM over 64-128 rotor revolutions
- Most people run in steady mode
- Or time-accurate for only 8-10 revs





Outline

- Numerical Approach
- Results
 - ❖ V22 *isolated* rotor in hover
 - Assess and demonstrate improvements in the CFD accuracy with rigid blades
 - ❖ Chaderjian and Buning, 67th AHS Forum, 2011
 - ❖ UH-60A *isolated* rotor in forward flight and hover
 - Demonstrate improvements with flexible blades
 - ❖ Chaderjian and Ahmad, AIAA 2011-3185
 - ❖ Chaderjian, 68th AHS Forum, 2012
 - ❖ Accoustics
 - Interesting preliminary results
- Conclusions
 - ❖ Summary paper of V22 and UH-60A
 - Chaderjian, ICCFD7-3506, July 2012,
 - ❖ <http://www.iccfd.org/iccfd7/proceedings.html>





Numerical Approach (OVERFLOW 2.2)

**Time-Dependent Navier-Stokes Equations
Solved Throughout the Entire Computational Domain**

$$\partial_\tau \hat{Q} + \partial_\xi (\hat{E} - \hat{E}_v) + \partial_\eta (\hat{F} - \hat{F}_v) + \partial_\zeta (\hat{G} - \hat{G}_v) = 0$$

$$\text{Where } \hat{Q} = J^{-1} [\rho, \rho u, \rho v, \rho w, e]$$

Pulliam-Chaussee Diagonal Algorithm

$$T_\xi^k \left[I + h \left(\delta_\xi \hat{\Lambda}_\xi^k - I \delta_{\xi\xi} \lambda_v^k(\xi) \right) \right] \hat{N} \left[I + h \left(\delta_\eta \hat{\Lambda}_\eta^k - I \delta_{\eta\eta} \lambda_v^k(\eta) \right) \right] \hat{P} \left[I + h \left(\delta_\zeta \hat{\Lambda}_\zeta^k - I \delta_{\zeta\zeta} \lambda_v^k(\zeta) \right) \right] (T_\zeta^{-1})^k \Delta \hat{Q}^k = -h R^{k,n}$$

$$\text{Where } R^{k,n} = \left(\frac{3\hat{Q}^k - 4\hat{Q}^n + \hat{Q}^{n-1}}{2\Delta t} \right) - \left[\delta_\xi (\hat{E}^k - \hat{E}_v^k) + \delta_\eta (\hat{F}^k - \hat{F}_v^k) + \delta_\zeta (\hat{G}^k - \hat{G}_v^k) \right]$$

$$\text{And } h = \left(\frac{2\Delta t \Delta \tau}{2\Delta t + 3\Delta \tau} \right)$$

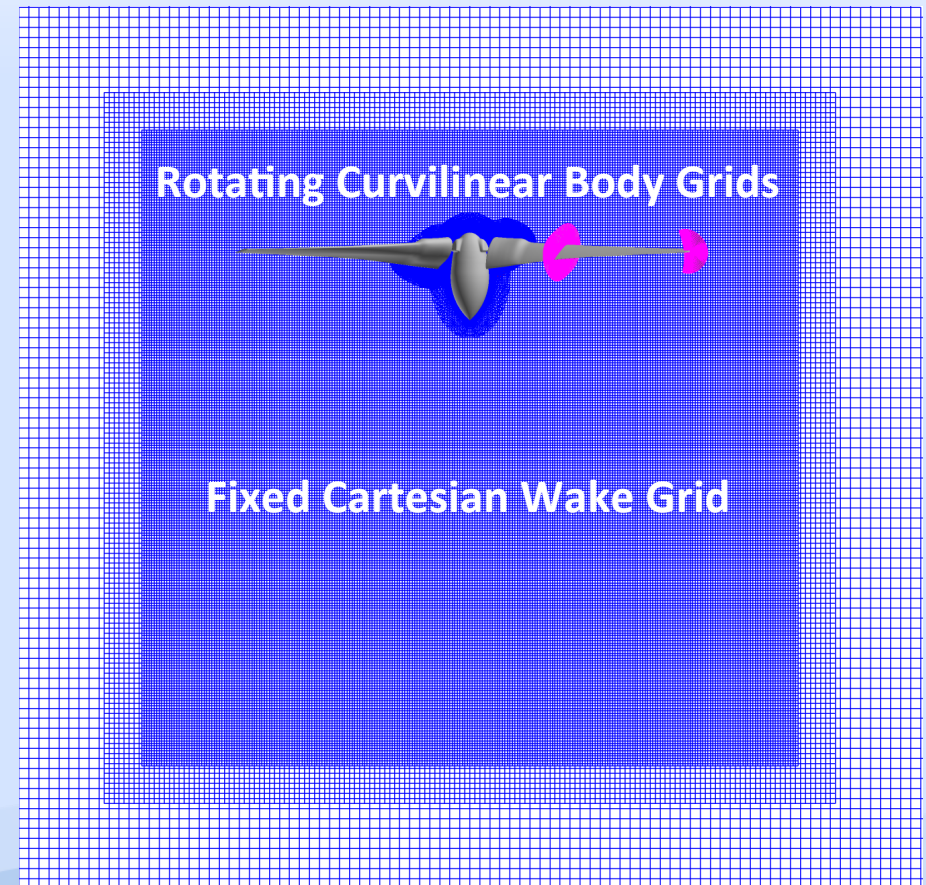
2nd-order Dual-Time Accuracy

- Physical time step: $\Delta t = \frac{1}{4}^\circ$ blade rotation
 - ❖ Time step index: n
- Pseudo time step: $\Delta \tau$
 - ❖ Subiteration index: k



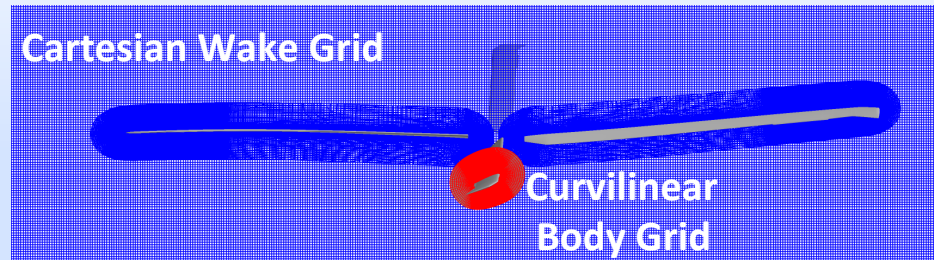
Numerical Approach (OVERFLOW 2.2)

- Overset grid system
- Up to 5th-order central spatial differences
- Spalart-Allmaras one-equation turbulence model with SARC rotational correction
- Dynamic adaptive mesh refinement (AMR) for the off-body (OB) Cartesian wake grids
- Flexible rotor blades: OVERFLOW loosely coupled with CAMRAD II (helicopter comprehensive analysis code)





OVERFLOW Spatial Accuracy



Convective Difference Operators

Cartesian Wake Grid Accuracy	Convective Central Difference Stencil	Artificial Dissipation
$O(\Delta X^2)$	$\delta_x^{(2)}$	$\sim (\Delta X^3) \delta_{x^4}$
$O(\Delta X^3)$	$\delta_x^{(4)}$	$\sim (\Delta X^3) \delta_{x^4}$
$O(\Delta X^4)$	$\delta_x^{(4)}$	$\sim (\Delta X^5) \delta_{x^6}$
$O(\Delta X^5)$	$\delta_x^{(6)}$	$\sim (\Delta X^5) \delta_{x^6}$
$O(\Delta X^6)$	$\delta_x^{(6)}$	$\sim (\Delta X^7) \delta_{x^8}$

- Curvilinear body-grid metrics: (ΔX^2)
 - Viscous terms on all grids: (ΔX^2)
- } 2nd- order formal accuracy



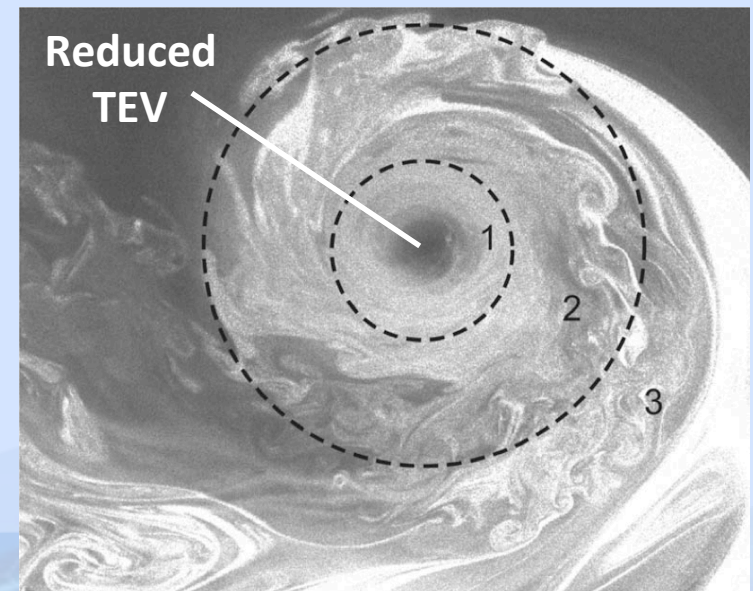
Spalart-Allmaras RANS Turbulence Model (SA-RANS)

$$\frac{D\tilde{\nu}}{Dt} = \underbrace{C_{b1}\tilde{\nu}\left(\Omega + \frac{\tilde{\nu}}{k^2 d^2} f_{v2}\right)}_{\text{Production}} - \underbrace{C_{w1}f_w\left(\frac{\tilde{\nu}}{d}\right)^2}_{\text{Dissipation}} + \underbrace{\frac{1}{\sigma}\left[\nabla\cdot((\mathbf{v} + \tilde{\nu})\nabla\tilde{\nu}) + C_{b2}(\nabla\tilde{\nu})^2\right]}_{\text{Diffusion}}$$

- **Production** and **dissipation** will play a key role in the accurate prediction of FM
- “ Ω ” is the vorticity magnitude
- “ d ” is the distance to the nearest body

- **Region 1 of vortex:** Stratified layers with little turbulent mixing and reduced fluid strain
 - ❖ SARC rotational correction reduces the turbulent eddy viscosity (TEV)

[Ramasamy et al., 2008]





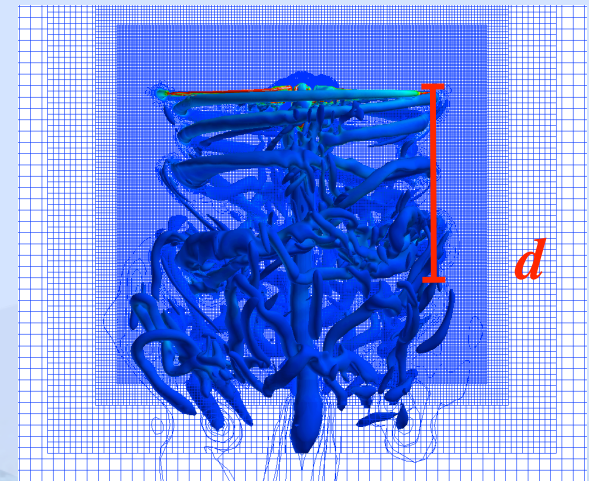
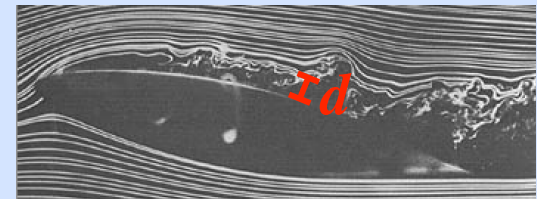
Spalart-Allmaras Detached Eddy Simulation (SA-DES)

$$\frac{D\tilde{\nu}}{Dt} = \underbrace{C_{b1}\tilde{\nu}\left(\Omega + \frac{\tilde{\nu}}{k^2\bar{d}^2}f_{v2}\right)}_{\text{Production}} - \underbrace{C_{w1}f_w\left(\frac{\tilde{\nu}}{\bar{d}^2}\right)^2}_{\text{Dissipation}} + \underbrace{\frac{1}{\sigma}\left[\nabla\cdot((\mathbf{v} + \tilde{\nu})\nabla\tilde{\nu}) + C_{b2}(\nabla\tilde{\nu})^2\right]}_{\text{Diffusion}}$$

DES provides a **more realistic** turbulent length scale

$$\bar{d} = \min(d, C_{DES}\Delta)$$

$$\Delta = \max(\Delta x, \Delta y, \Delta z)$$



- Viewed as a hybrid model
 - ❖ RANS in boundary layer
 - ❖ LES outside of boundary layer (implicit filter)
- Turbulent structures are resolved if the mesh is refined
- If the mesh is not refined
 - ❖ Rational way to reduce TEV and vortex diffusion
 - ❖ Don't need ad-hoc methods, e.g., vortex confinement or the Euler equations
- The RANS distance function "d" was responsible for the wake disappearing in the earlier movie
 - ❖ The DES length scale fixes this problem

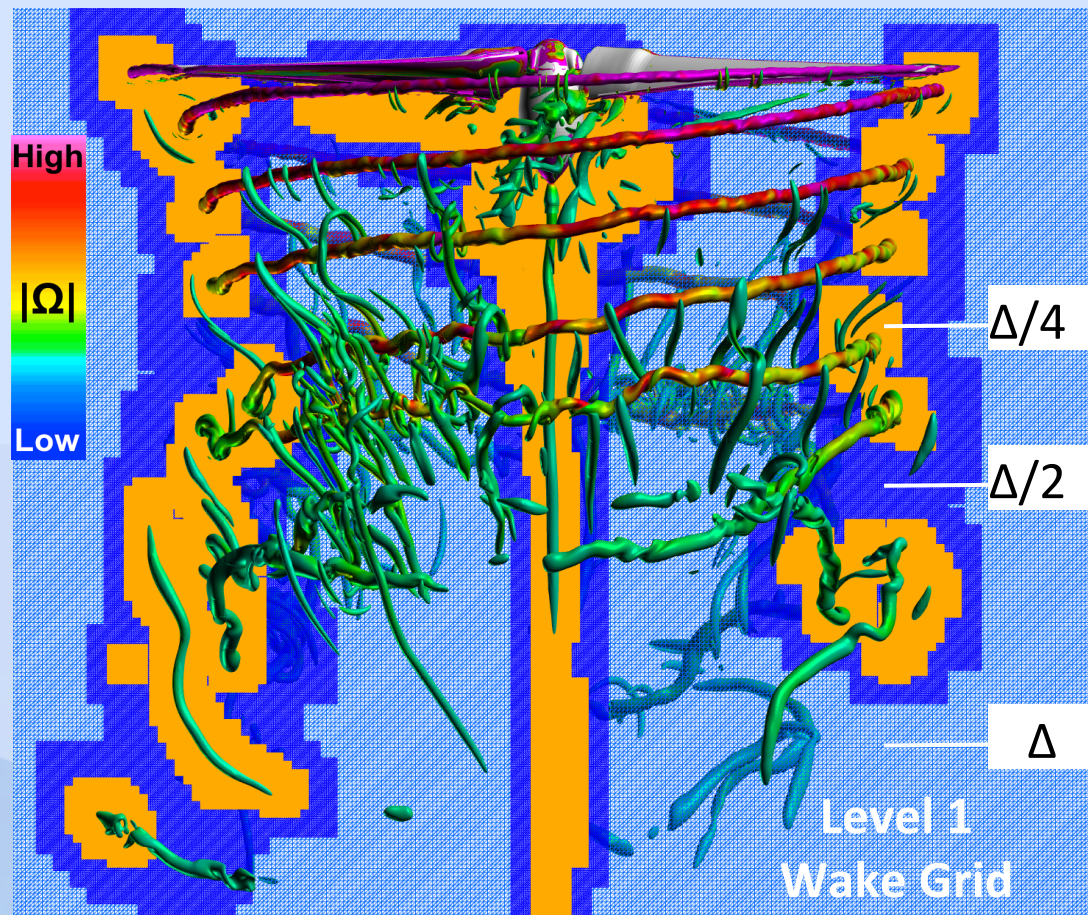
SA-DES with SARC provides a comprehensive model for turbulent rotor wakes



OVERFLOW's Dynamic Adaptive Mesh Refinement (AMR)

Two Refinement Levels: $\Delta=10\%$, 5% , and $2.5\%c_{tip}$

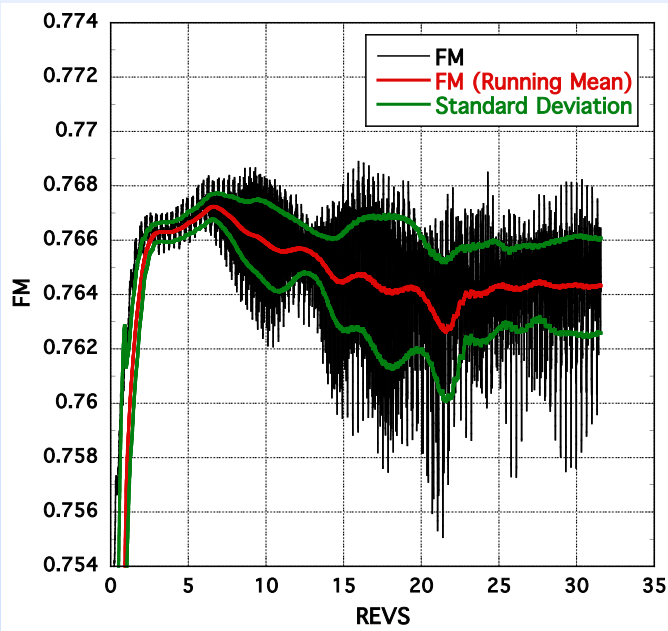
- Refined Cartesian grids are automatically added to or removed from the baseline Level-1 wake grid
- User specified thresholds based on the vorticity magnitude
- Refinement padding: No interpolation in high-gradient regions





Computing the FM

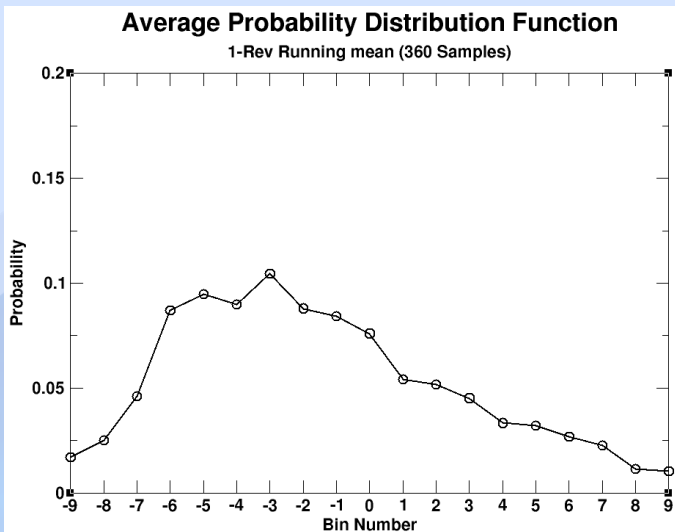
$M_{tip}=0.625, \theta=10^\circ, Re=2.1$ million



$$\overline{FM} = \frac{1}{N_s + 1} \sum_{n=N_s}^n \left(\frac{C_T^{3/2}}{\sqrt{2}C_Q} \right); \text{ Running Mean } (N_s \text{ Steps/Rev})$$

$$\overline{\overline{FM}} = \frac{\overline{C_T}^{3/2}}{\sqrt{2}\overline{C_Q}}; \text{ Use Running Means } \overline{C_T} \text{ and } \overline{C_Q}$$

- OVERFLOW FM is computed as a running mean
 - ❖ 1 standard deviation ~ 0.001 (3rd digit significant)
 - ❖ Assumes a normal distribution (68% samples in one σ)
 - ❖ Actual distribution is skewed to lower values



- Difference in two running means not significant
- Running mean provides
 - ❖ Monitor convergence
 - ❖ Quantifies FM variation
- Two digit accuracy in about 10 revs
- Three digit accuracy in 20-30 revs



OVERFLOW Results for V22 TRAM in Hover

Rotor Blades Treated as Rigid

V22 Osprey
Helicopter Mode



Tilt Rotor Aeroacoustics
¼-Scale Model (TRAM)

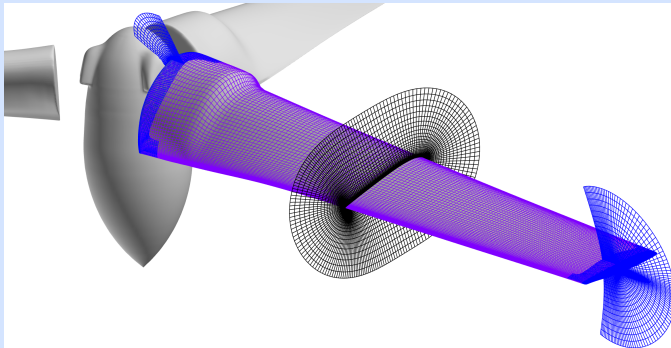




OVERFLOW Results for V22 TRAM in Hover

Baseline Overset Grid System: 35 Million Grid Points

Near Body (NB) O-Grids
Blunt Trailing Edge, $Y^+ < 0.4$



Off-Body (OB) Cartesian Grids





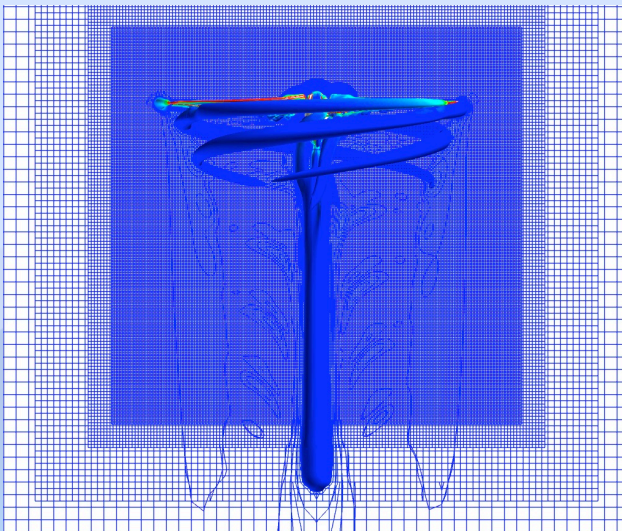
Effect of Spatial Differencing on FM

TRAM Hover: $M_{tip}=0.625$, $\theta=14^\circ$, $Re=2.1$ million
SA-RANS Turbulence Model with SARC

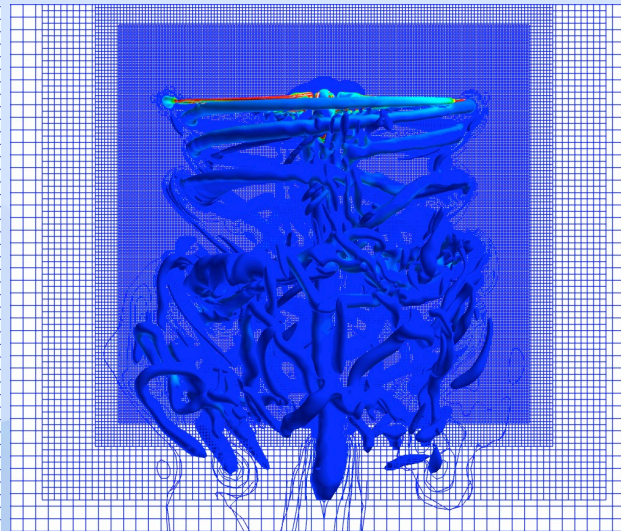
$$FM_{EXP}=0.779$$

- 5th-order differences improves upon the 3rd-order result
 - ❖ Improved prediction of FM
 - ❖ More detailed vortex wake (less diffusion)
- Near-body accuracy is crucial to accurately predict FM
 - ❖ Off-body accuracy is not that important

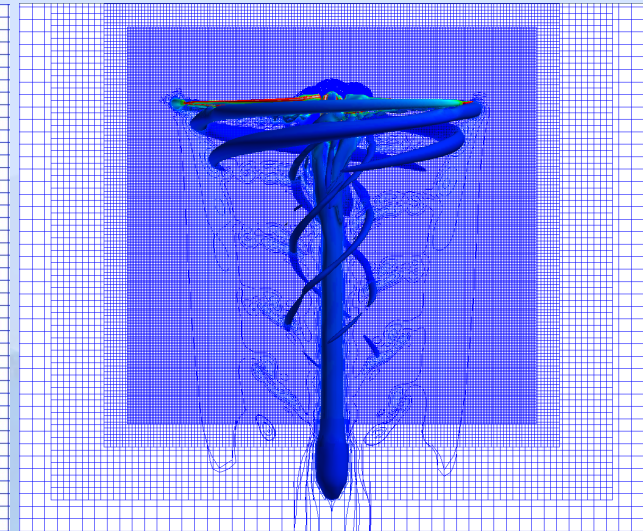
3rd-Order
FM=0.733, 6% Error



5th-Order
FM=0.777, 0.3% Error



3rd/5th-Order NB/OB
FM=0.733, 6% Error





Effect of Grid Resolution/Accuracy on FM

TRAM Hover: $M_{tip}=0.625$, $\theta=14^\circ$, $Re=2.1$ million

- Fig. 2 is better than Fig. 1
- Fig. 3 is better than Fig. 2
- It is again seen that near-body accuracy is crucial to accurately predict FM
 - ❖ Off-body accuracy is not that important

FM_{EXP}=0.779

(Fig. 1)

3rd-Order, Holst/Pulliam
Body: 1X; Wake 1X
FM=0.73, 6% Error



(Fig. 2)

3rd-Order Holst/Pulliam
Body: 2X; Wake 2X
FM=0.77, 0.9% Error

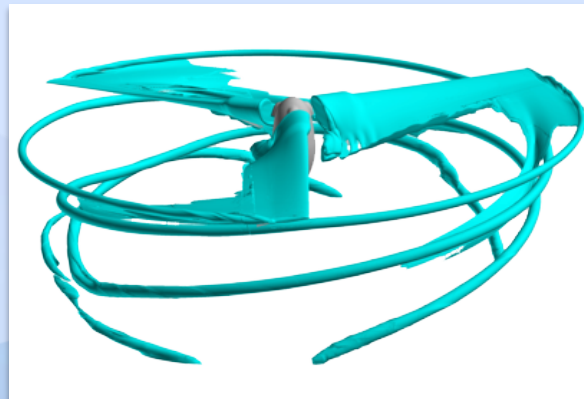
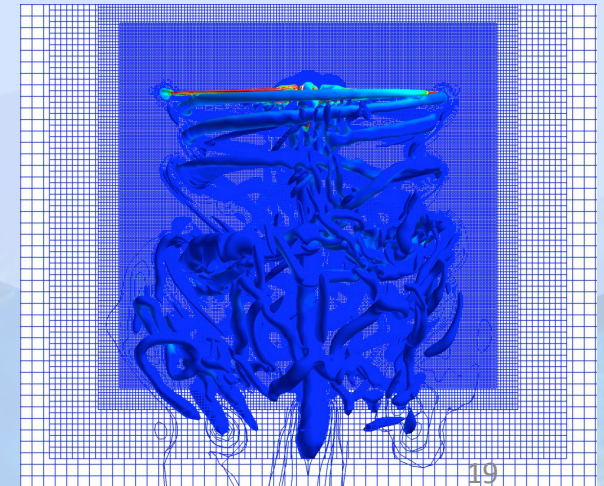


(Fig. 3)

5th-Order, Chaderjian
Body: 2X; Wake 1X
FM=0.777, 0.3% Error



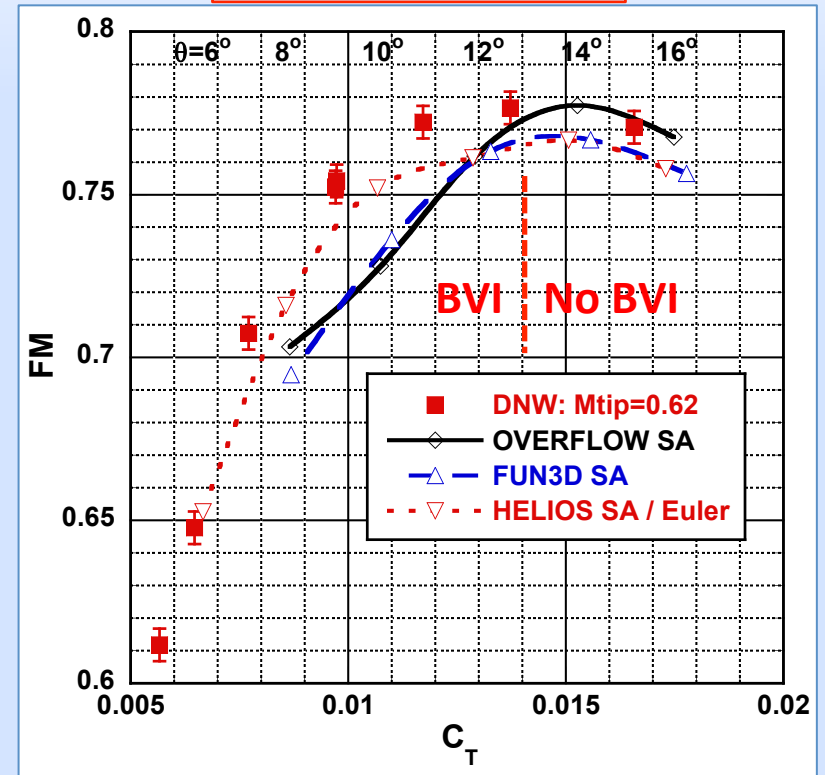


Baseline TRAM Collective Sweep Results

$M_{tip}=0.625$, $6^\circ \leq \theta \leq 16^\circ$, $Re=2.1$ million

RANS Length Scale

- OVERFLOW FM agrees with experiment at high collectives
 - ❖ Under predicts FM for lower collectives
- FUN3D/HELIOS FM under-predicts experiment for all collectives
- All codes under-predict FM when there is BVI
- Two observations
 - ❖ Significant BVI when $\theta < 14^\circ$
 - ❖ TEV is elevated for BVI cases
- Traced to RANS turbulent length scale

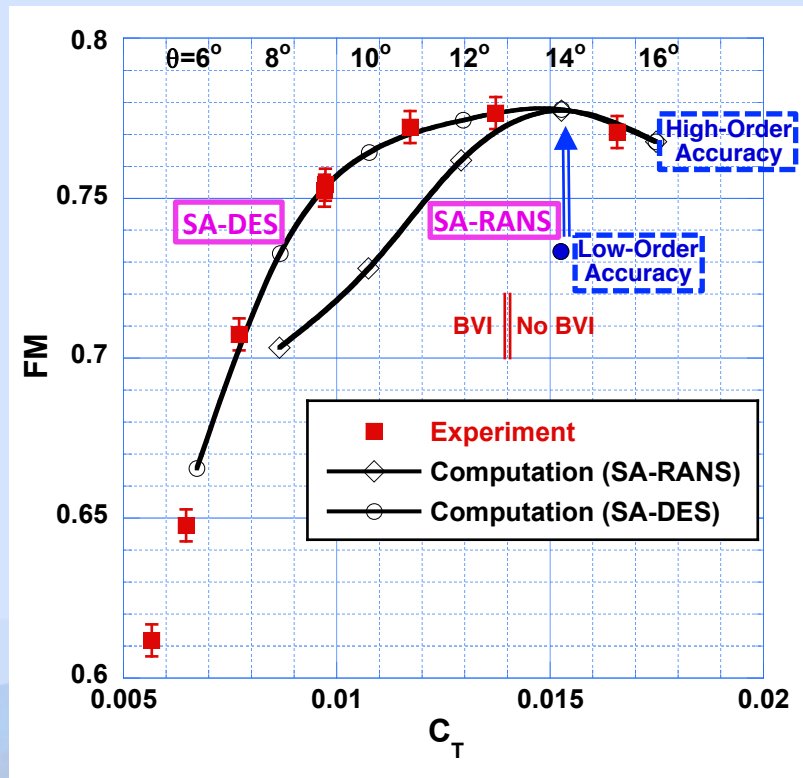




Baseline V22 TRAM Figure of Merit (FM) Results (RANS and DES Turbulence Models)

- FM (hover efficiency) is now within experimental error
- High-order accuracy important for all blade angles
- DES turbulence model approach important for BVI cases

Tilt Rotor Aeroacoustics 1/4-Scale Model (TRAM)



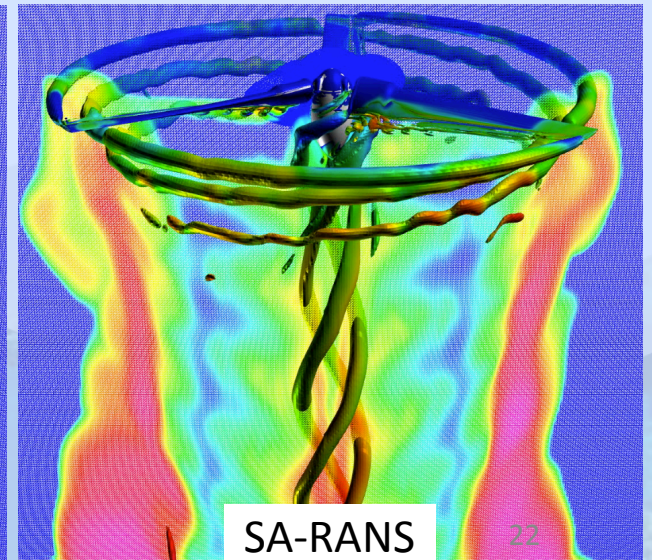
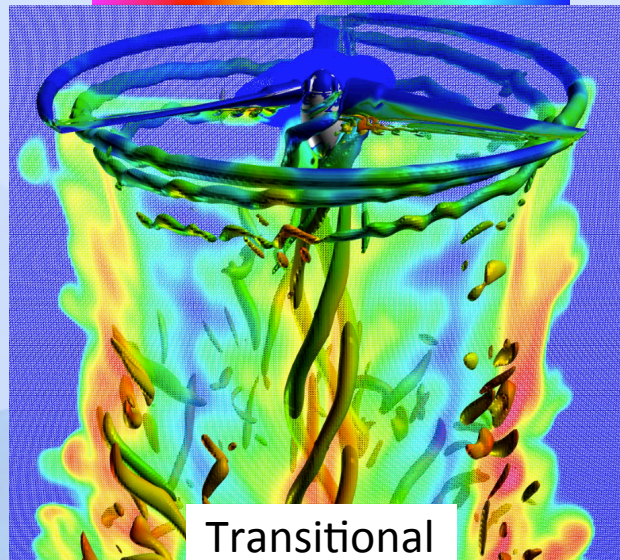
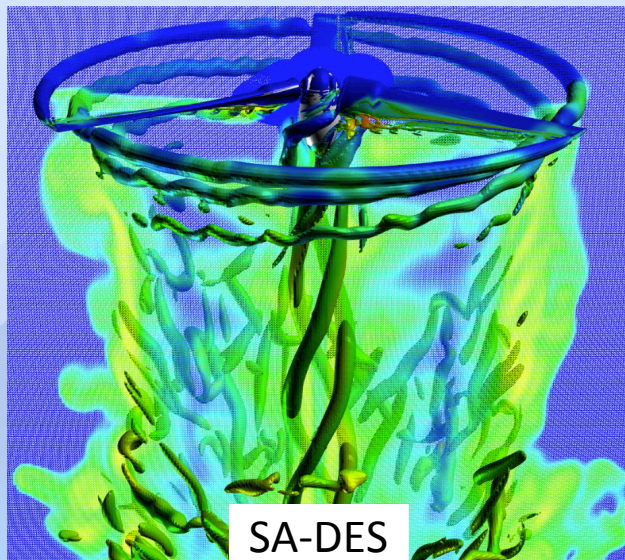
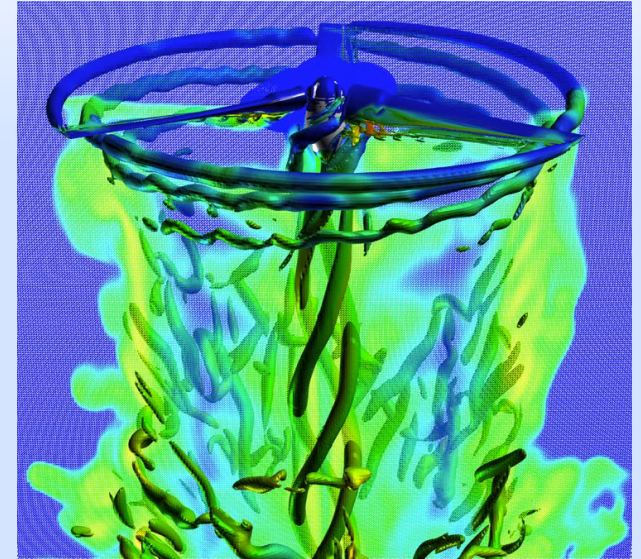


Progression of TEV from SA-DES to SA-RANS

TRAM Hover: $\theta=10^\circ$, Strong BVI

- Start with SA-DES, then switch to SA-RANS
- TEV grows most rapidly deep with the wake, but eventually affects all of the wake (10 revs)
- Wake TEV infiltrates the blade boundary layers with BVI, reducing the FM
 - ❖ C_T about the same
 - ❖ C_Q increases significantly

$$FM = \frac{C_T^{3/2}}{\sqrt{2}C_Q}$$





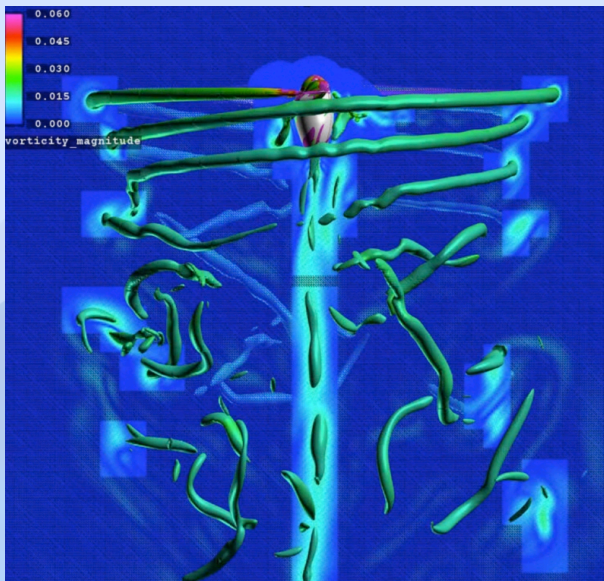
Recall the First Attempt with AMR Using SA-RANS

TRAM Hover: $\theta=14^\circ$, Strong BVI

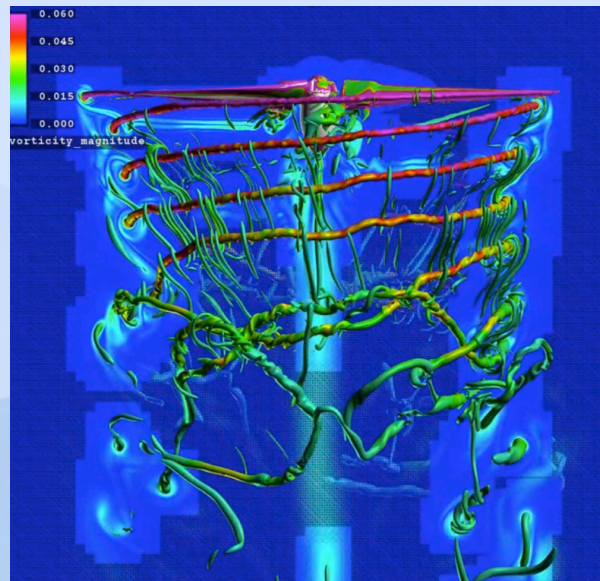
- The first AMR movie showed the eventual destruction of the lower wake
 - ❖ The improved vortex resolution also increased turbulent production
 - ❖ The large RANS length scale kept the turbulent dissipation too low
 - ❖ The imbalance between production and dissipation resulted in a high TEV in the lower wake
- The resulting high TEV in the lower wake diffused the lower wake vortices

$$\frac{D\tilde{v}}{Dt} = \underbrace{C_{b1}\tilde{v}\left(\Omega + \frac{\tilde{v}}{k^2 d^2} f_{v2}\right)}_{\text{Production}} - \underbrace{C_{w1}f_w\left(\frac{\tilde{v}}{d^2}\right)^2}_{\text{Dissipation}} + \underbrace{\frac{1}{\sigma}\left[\nabla\cdot((v+\tilde{v})\nabla\tilde{v}) + C_{b2}(\nabla\tilde{v})^2\right]}_{\text{Diffusion}}$$

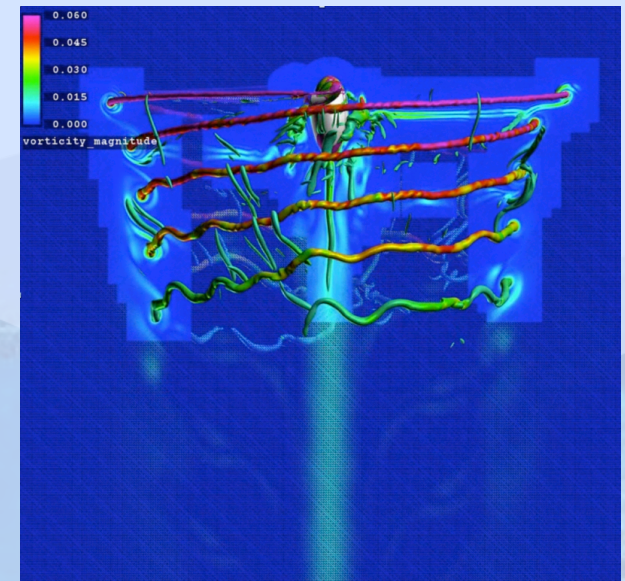
Before AMR



During AMR



After AMR



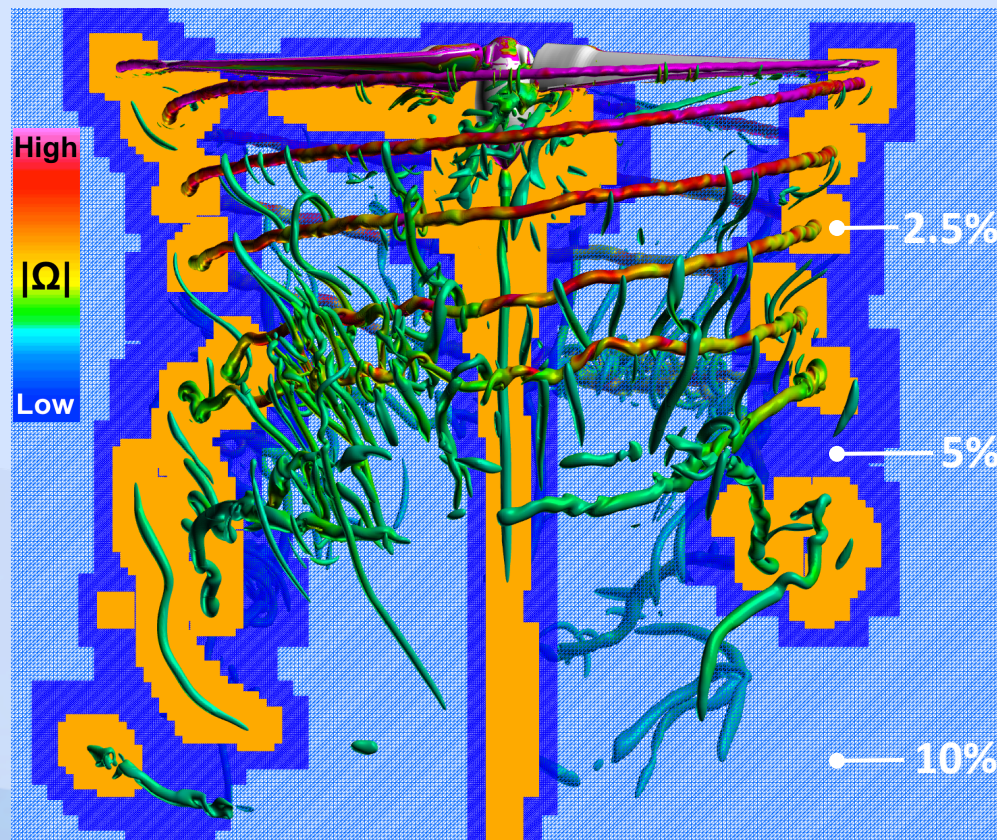


Adaptive Mesh Refinement (AMR) in OVERFLOW

All Remaining AMR Uses SA-DES with SARC

- Baseline: ($\Delta=10\% c_{tip}$) No AMR-Uniform
- AMR1: ($\Delta=10\%$, $5\% c_{tip}$)
- AMR2: ($\Delta=10\%$, 5% , $2\% c_{tip}$)

Example AMR2

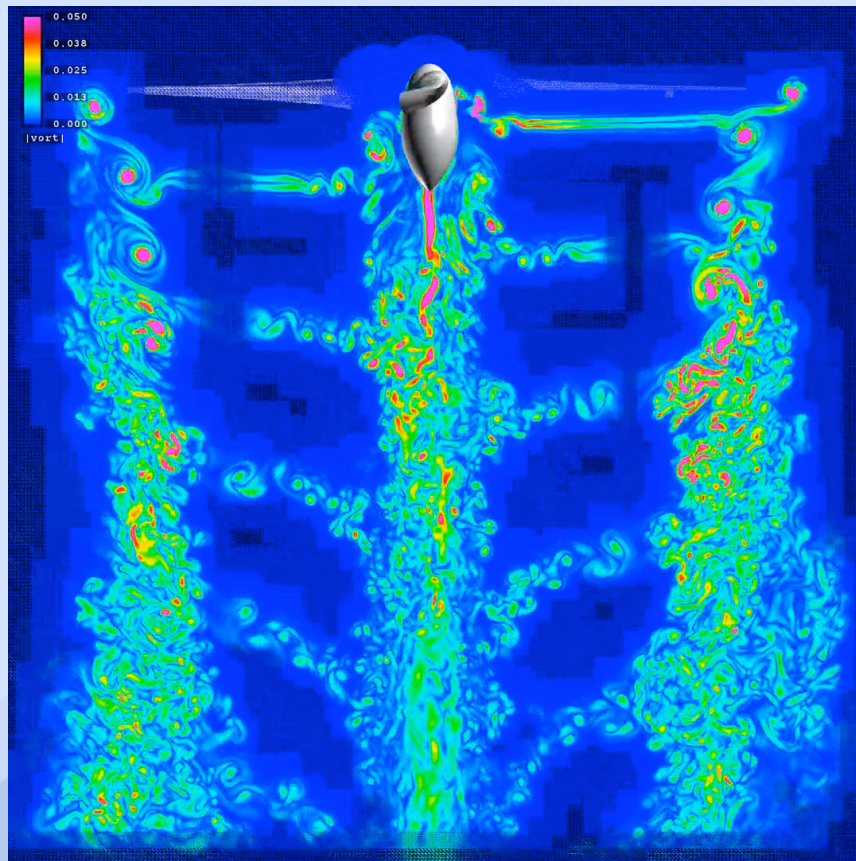




Adaptive Mesh Refinement (AMR) in OVERFLOW

SA-DES, $\theta=14^\circ$, ($\Delta=10\%$, 5% , $2.5\%c_{tip}$)

Y=0 Cutting Plane Showing AMR



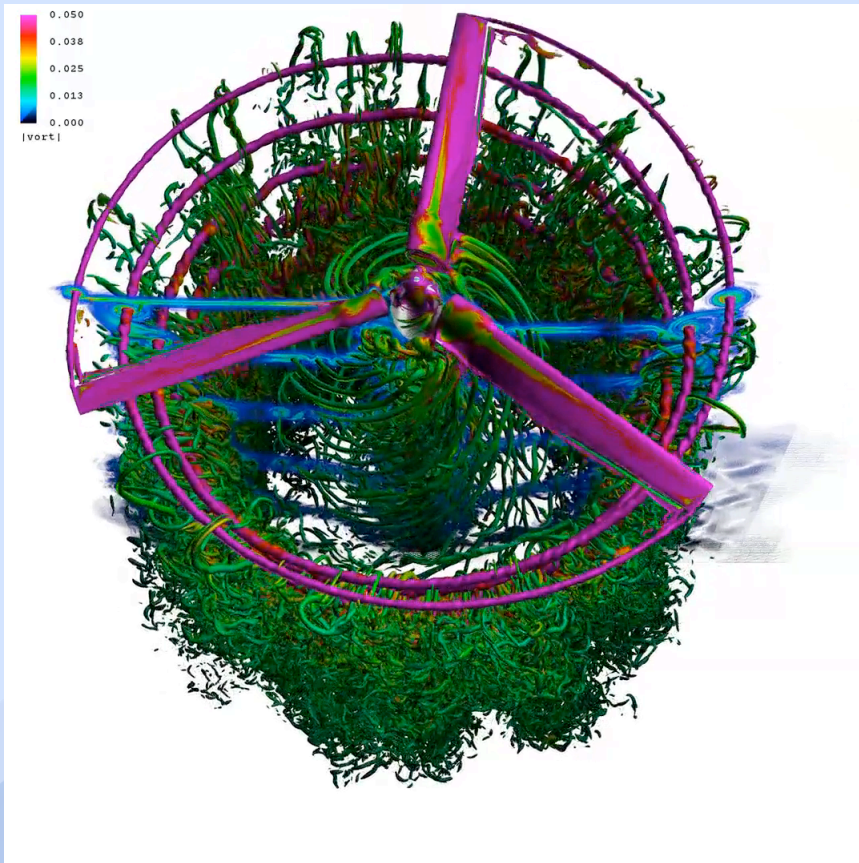
- Started from baseline result (20 revs) and run 10 more revs
- All vortical structures are detected and refined
- AMR vortices are stronger and have smaller diameters than the baseline result
- Turbulent structures in the lower wake
- About 14,000 grids, 670 million grid points



Dynamic AMR in OVERFLOW

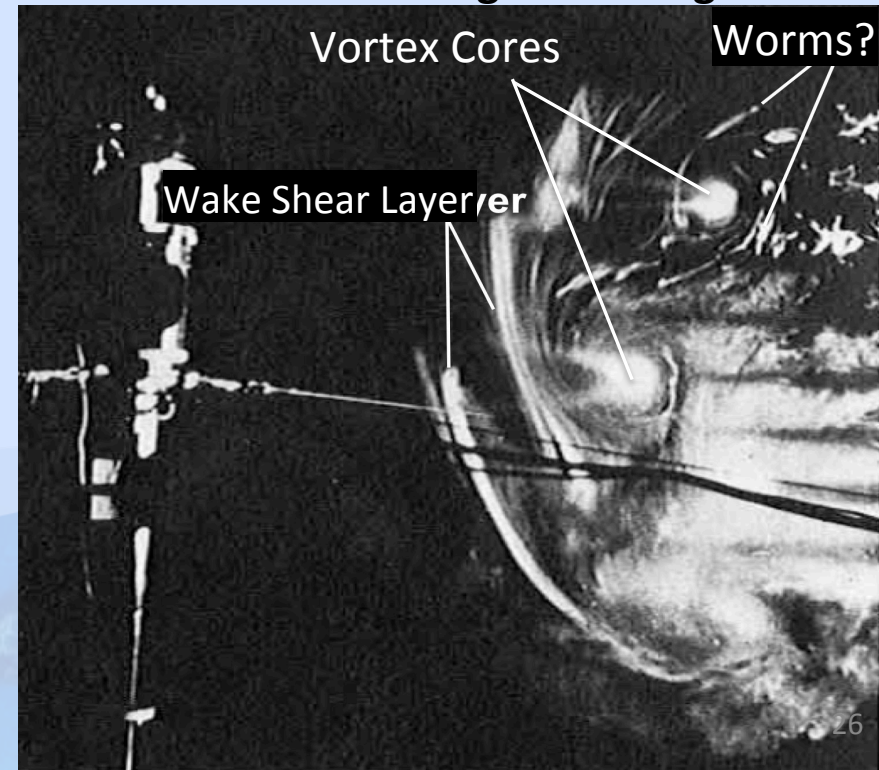
SA-DES, $\theta=14^\circ$, ($\Delta=10\%$, 5% , $2.5\%c_{tip}$)

Overhead View



- Worm-like vortical structures appear in the lower wake
- $FM_{OVERFLOW}=FM_{EXP}=0.779$
- Experimental evidence of worms (Gray 1956)
- But what is the source of the worms?

Smoke Flow for a Single Rotating Blade

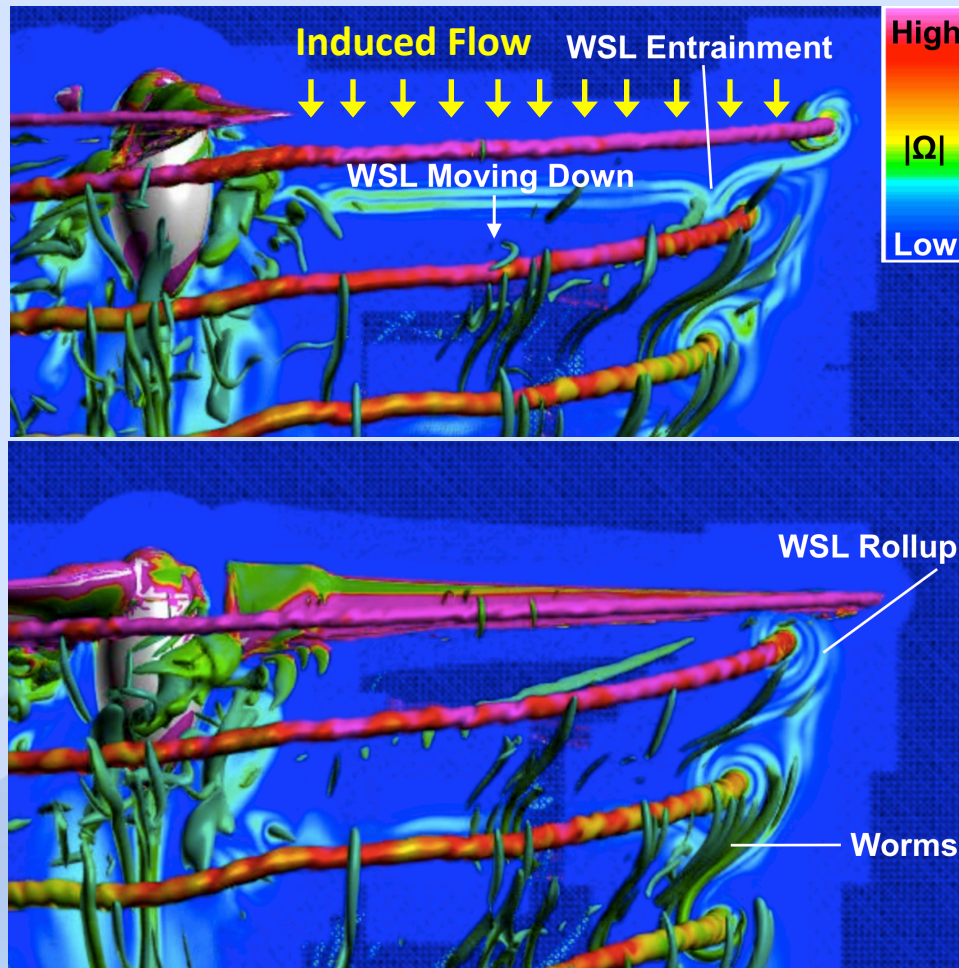




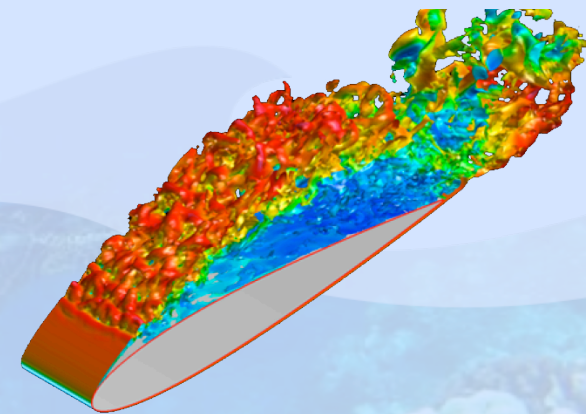
Physical Mechanism for Vortical Worms

SA-DES, $\theta=14^\circ$, ($\Delta=10\%$, 5% , $2.5\%c_{tip}$)

Y=0 Cutting Plane
Vortices Rendered with q-Criterion



- There is relative motion between the Wake Shear Layer (WSL) and the vortices due to an induced flow
- Vortical worms form through a vortex stretching process
- Worms roll up and are entrained into the vortices
- There are more worms in the lower wake due to more WSL/vortex interaction
- Similar turbulent structures are common in large eddy simulation (LES)

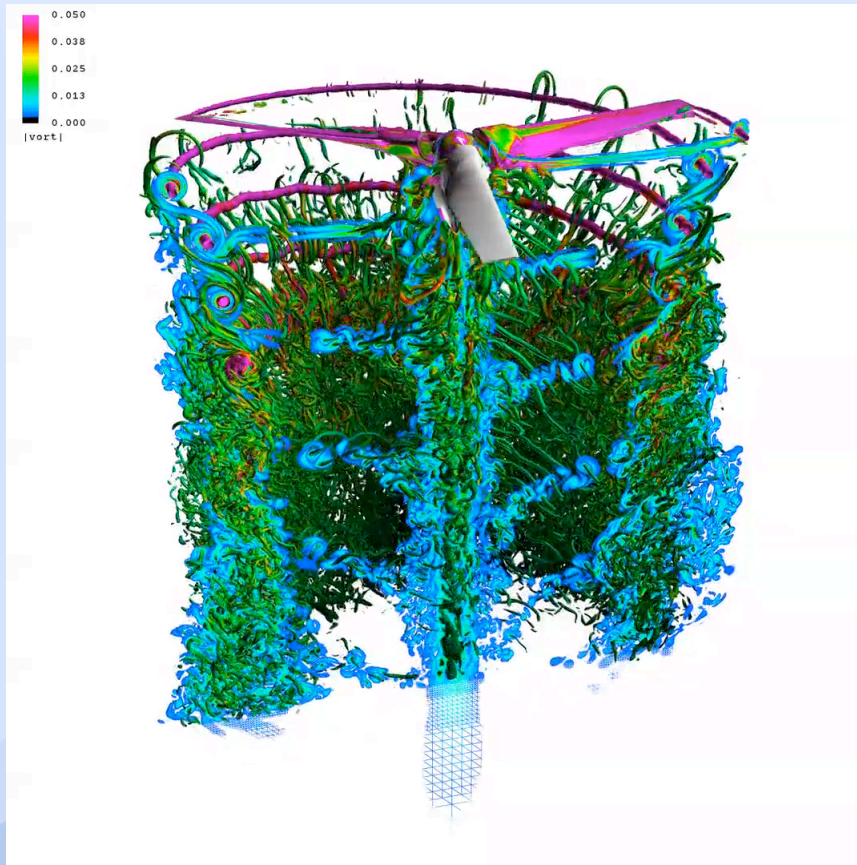




Physical Mechanism for Vortical Worms

SA-DES, $\theta=14^\circ$, ($\Delta=10\%$, 5%, 2.5% c_{tip})

Cut-Away View

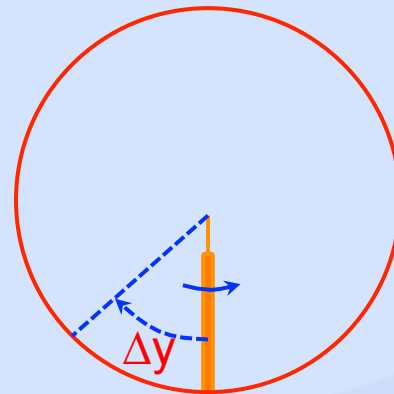
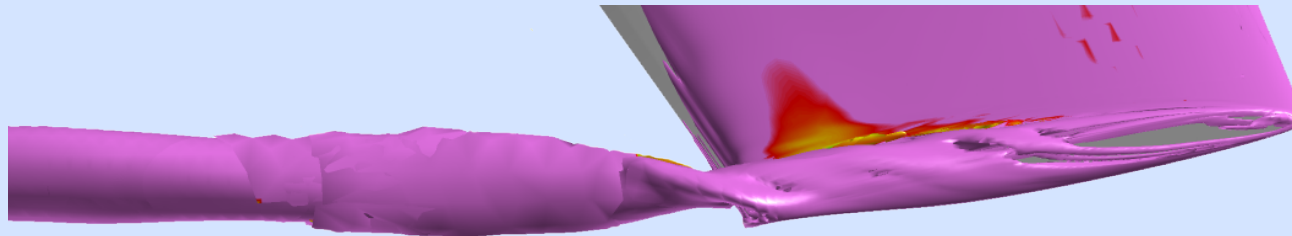


- Note WSL is descending
- WSL is constantly stretched and pulled towards vortex cores
- Worms are more prolific in the lower wake, due to more WSL encounters with the vortices
- AMR not needed to predict FM
- Difference within one standard deviation

Collective	Baseline FM	AMR FM	Difference
10° (BVI)	0.764	0.763	-0.001
14° (No BVI)	0.778	0.779	0.001



Is the Size of the Computed Vortex Core Realistic?



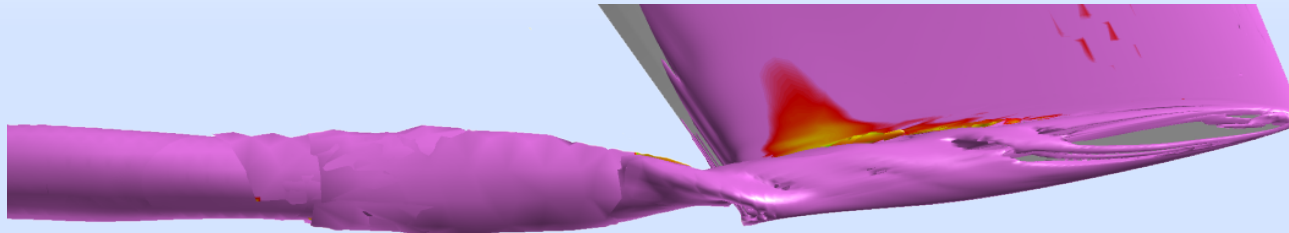
Wake Age



Formation of Tip Vortex and Core Growth

TRAM Hover: $M_{tip}=0.625$, $\theta=14^\circ$, $Re=2.1$ million, DES

AMR2: $\Delta=10\%$, 5% , $2.5\%c_{tip}$



Near-Body / Off-Body Grid Overlap

- Vortex is non-circular very near the tip
 - ❖ Upper/lower boundary layers resemble a rope braid
- Vortex core grows with **wake age** (Δy)
- Near-body and off-body grids well matched



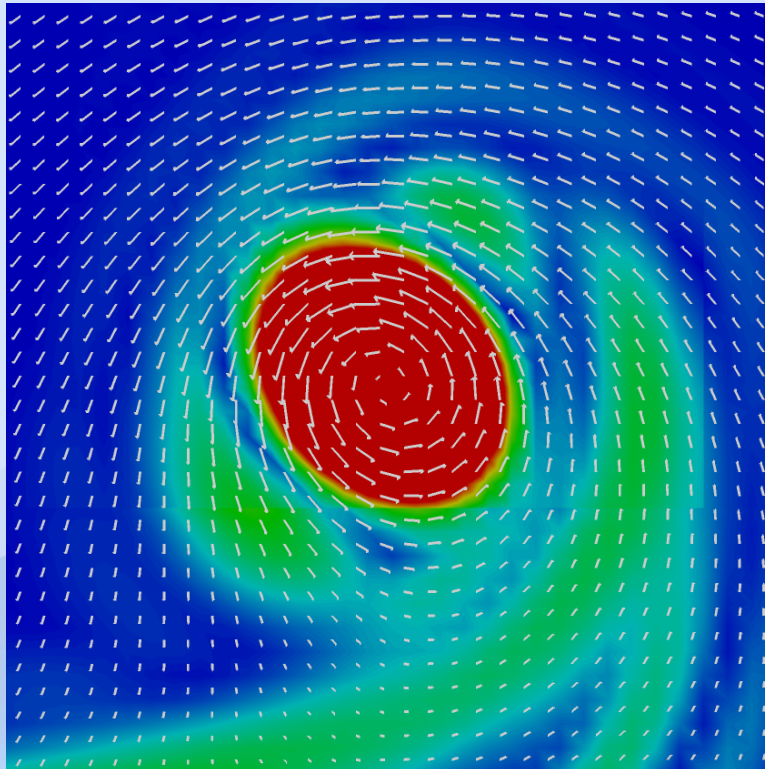
Vortex Cross-Flow Velocity Vectors

TRAM Hover: $M_{tip}=0.625$, $\theta=14^\circ$, $Re=2.1$ million, SA-DES

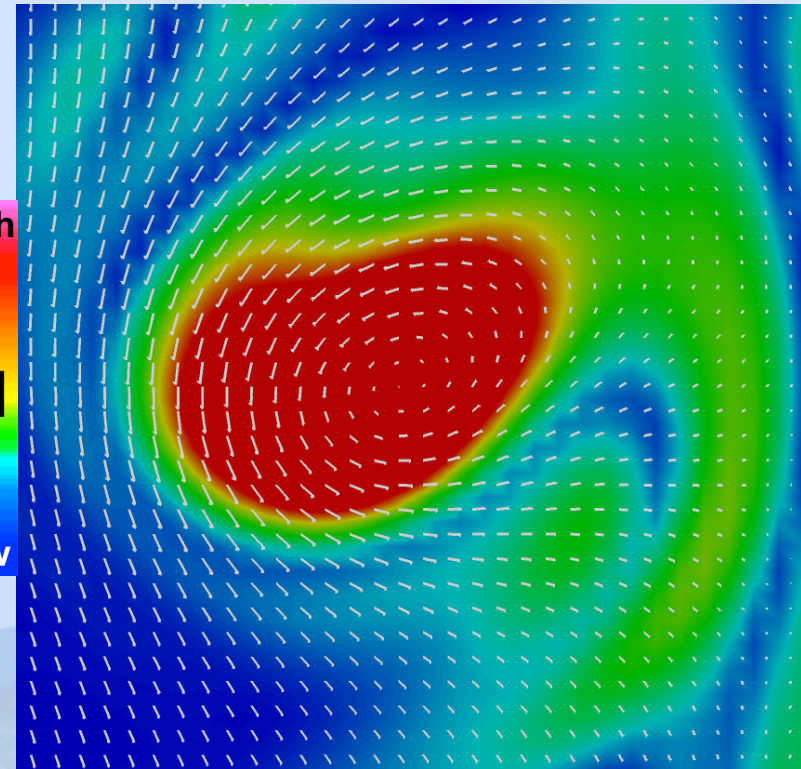
AMR2: $\Delta=10\%$, 5% , $2.5\%c_{tip}$

- Note distortion of “circular” vortex, even at an early wake age
- Shear-layer entrainment complex due to vortical worms and vortex pairing

Wake Age = 30°



Wake Age = 390°



High
 $|\Omega|$
Low

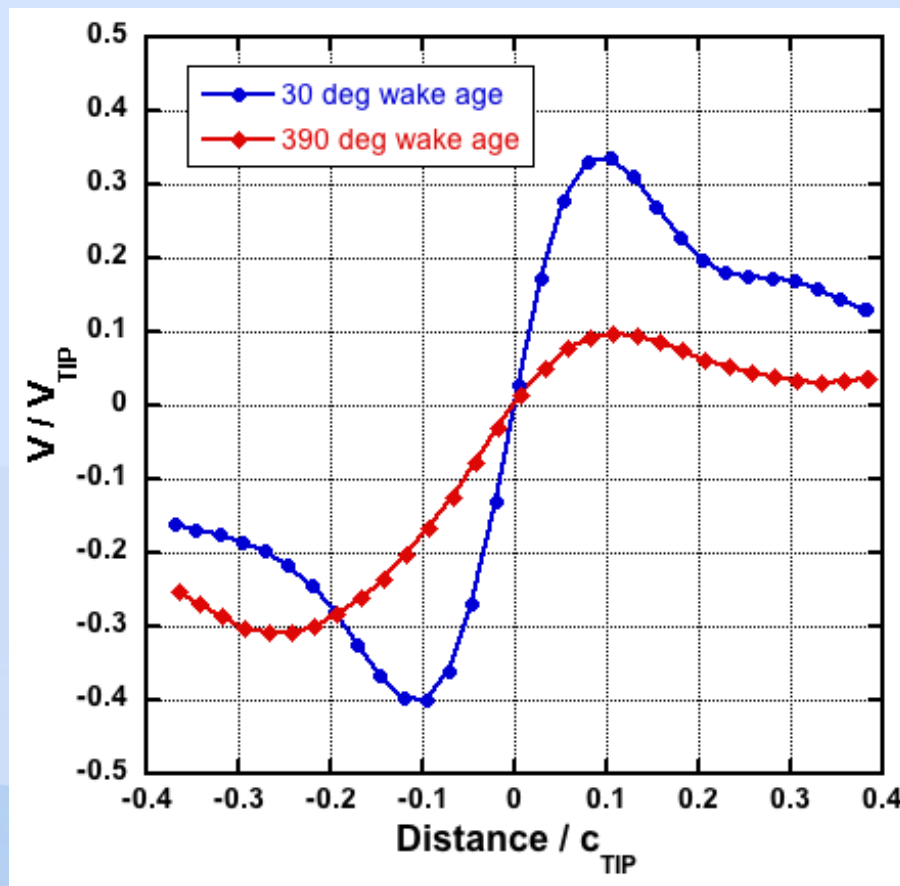


Vortex Cross-Flow Velocity Vectors

TRAM Hover: $M_{tip}=0.625$, $\theta=14^\circ$, $Re=2.1$ million, SA-DES

AMR2: $\Delta=10\%$, 5% , $2.5\%c_{tip}$

- Note distortion of “circular” vortex
- Symbols indicate grid-point locations
 - ❖ Near and far wake-age vortices have 8 and 14 grid cells, respectively

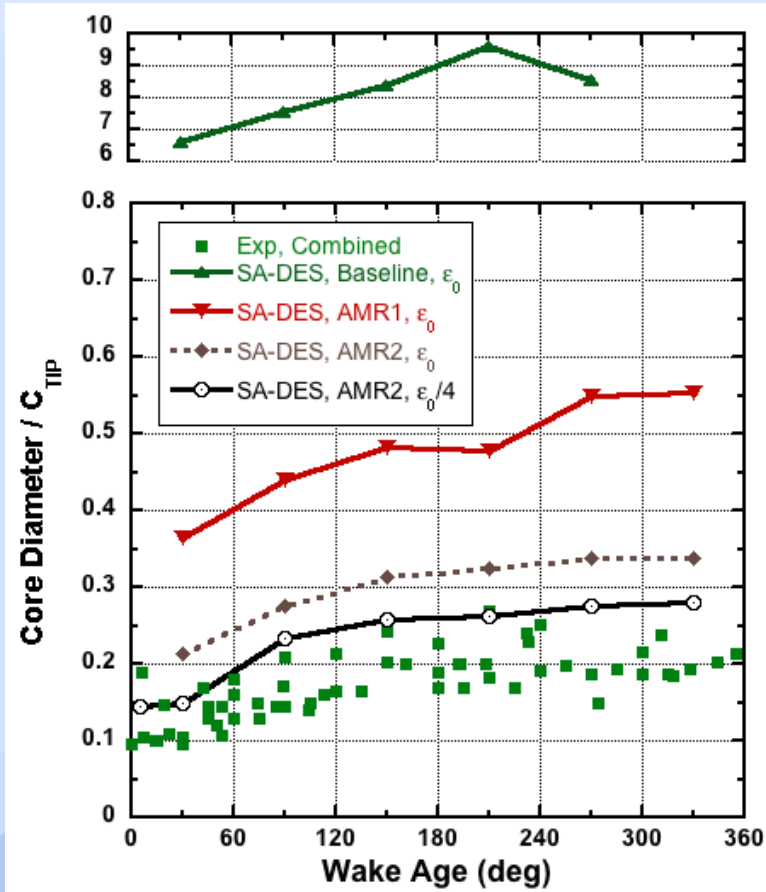




Vortex Core Diameter Growth With Wake Age

TRAM Hover: $M_{tip}=0.625$, $\theta=14^\circ$, $Re=2.1$ million, DES

Vortex Core Growth with wake Age



- Vortex core growth with wake age improves with off-body resolution
- AMR2 resolution with reduced artificial dissipation in good agreement with experiment
- Vortex growth rate (regression exponent) in good agreement with experiment

Regression Curve Fit

$$\left(D \sim \Delta\psi^P : \Delta\psi \geq 30^\circ \right)$$

Case	Finest Grid Spacing C_{tip}	Regression Exponent
Baseline	10%	0.15
AMR1	5%	0.17
AMR2	2.5%	0.20
AMR2 Low Dis	2.5%	0.26
Experiment	NA	0.25

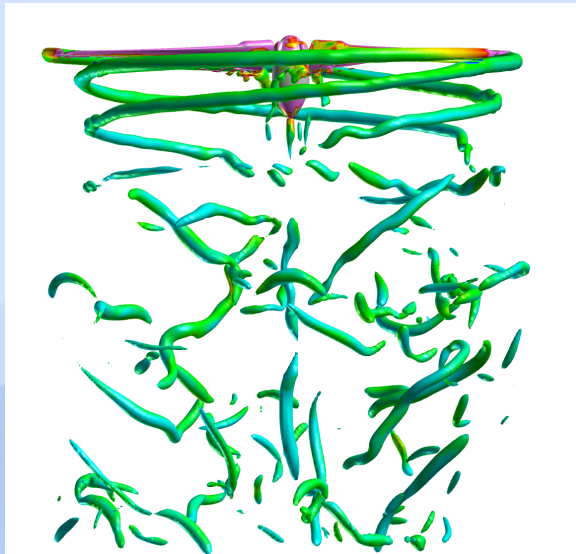


Progression of Wake Complexity with AMR Refinement

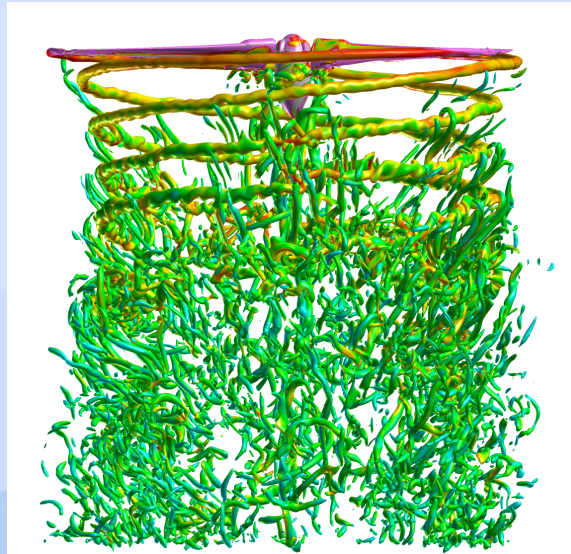
TRAM Hover: $M_{tip}=0.625$, $\theta=14^\circ$, $Re=2.1$ million, DES

- Baseline has no worms
- AMR2 has more smaller worms than AMR1
 - ❖ Expected, as DES resolves more turbulent scales
- Largest AMR2 worms are 15% smaller than than AMR1 worms
- Both AMR1 and AMR2 worm vorticity about 7% tip vortex
- Largest worms are realistic is size, though more refinement is needed

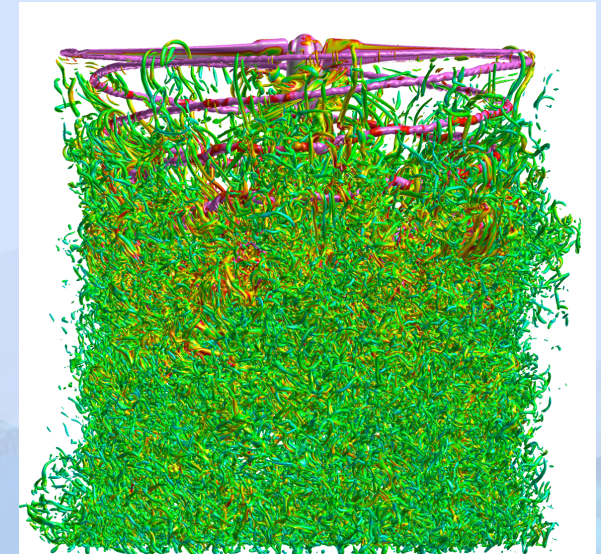
Baseline



AMR1



AMR2



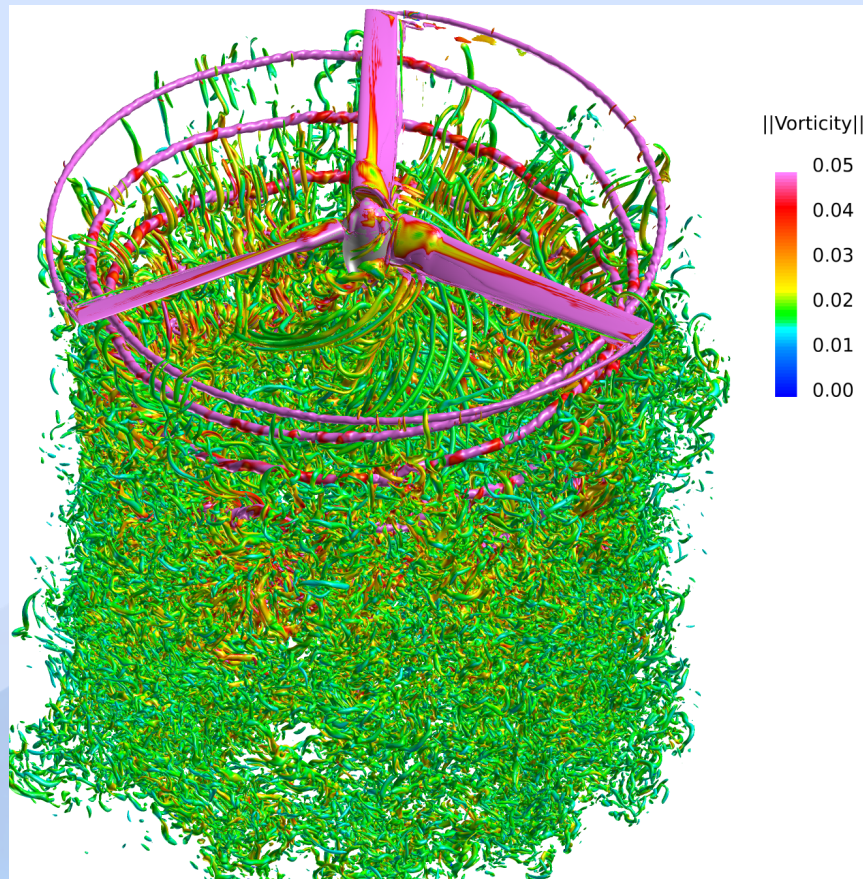


Comparison of AMR2 Wake with Uniform Grid Spacing

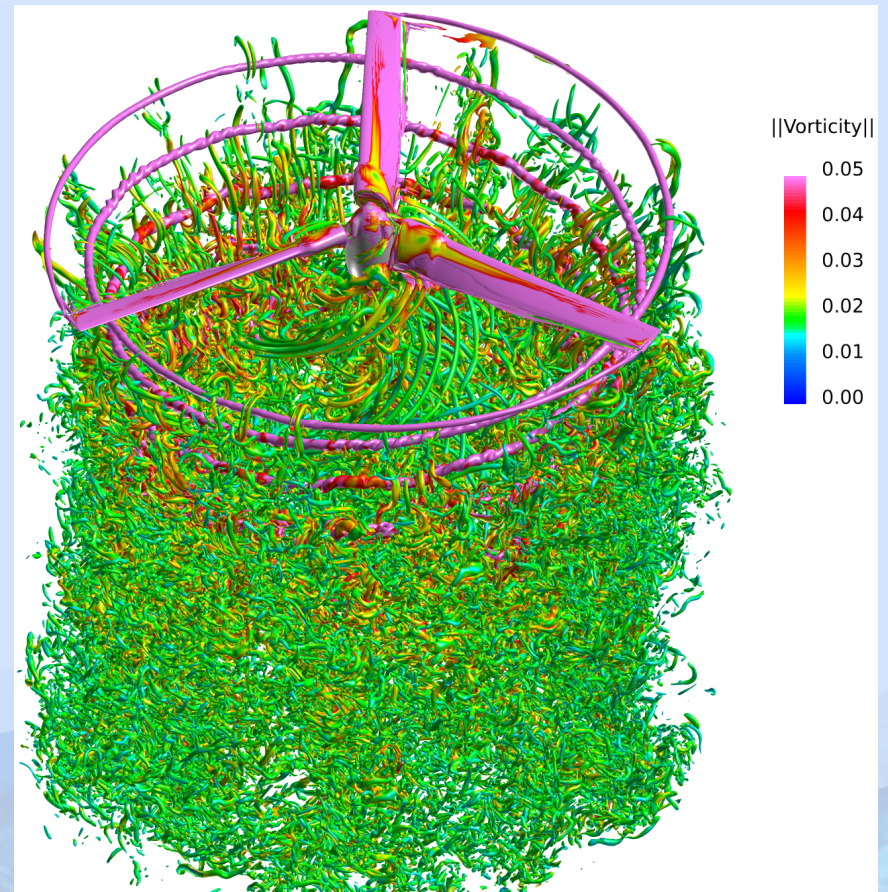
TRAM Hover: $M_{tip}=0.625$, $\theta=14^\circ$, $Re=2.1$ million, DES

No significant difference between AMR2 and uniform mesh vorticity contours

$\Delta=10\%$, 5% , $2.5\%c_{tip}$
670 Million Grid Points



Uniform $\Delta=2.5\%c_{tip}$
1.3 Billion Grid Points





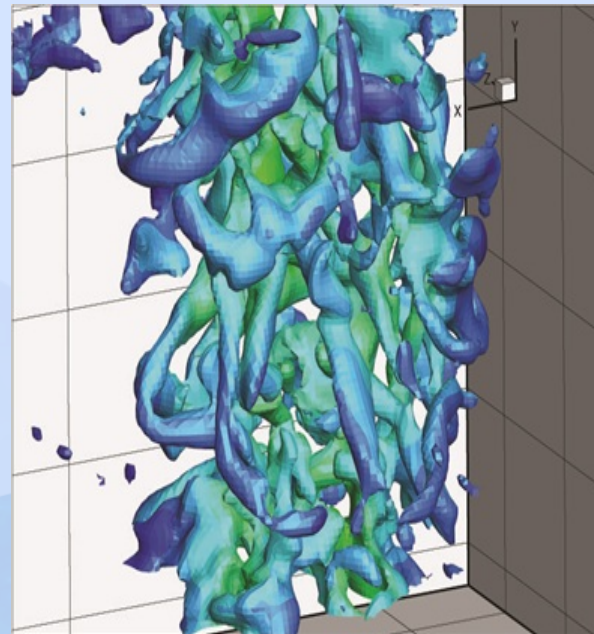
The Challenge for Experiment

- Measure FM to the same precision as CFD
- Experimentally observe the turbulent worms predicted by CFD
 - ❖ Tomographic Particle Image Velocimetry (tomo-PIV) is a new method under development that looks promising

Tomo-PIV of a Turbulent Jet

4 cameras (1200 fps)

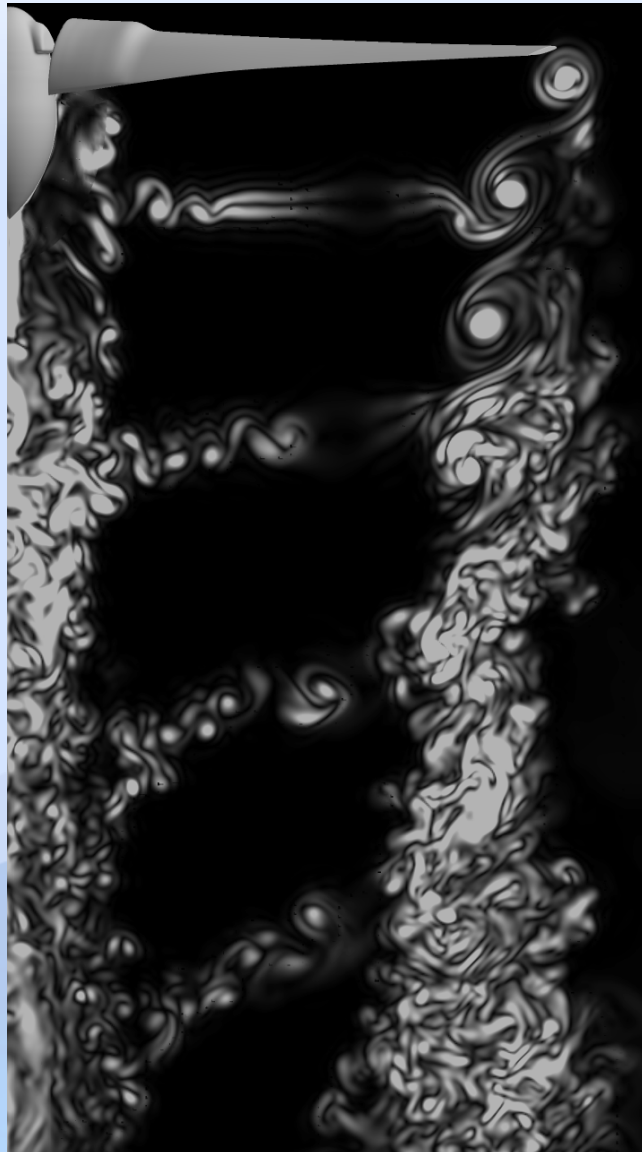
Casey & Sakakibara



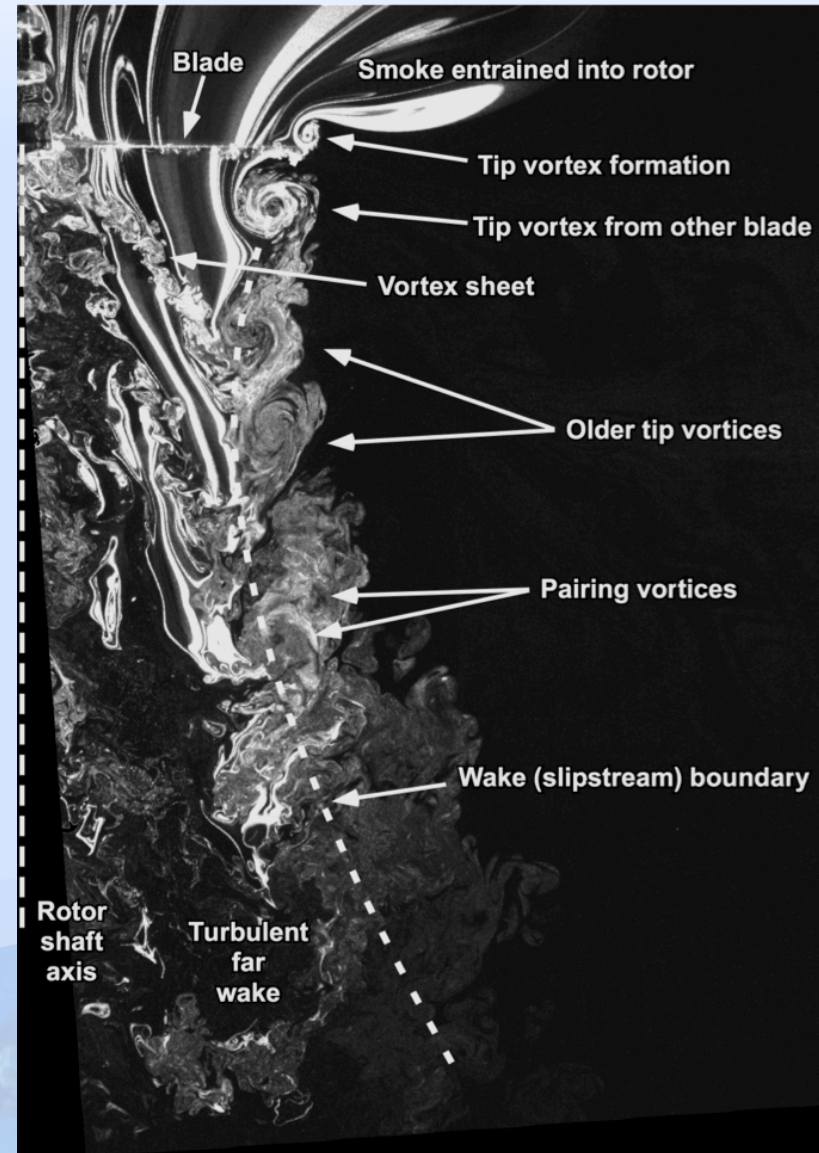


Numerical and Experimental Rotor Wakes

CFD: TRAM 3-Bladed Rotor



Experiment: 2-Bladed Rotor, Sydney et.al





Summary of TRAM FM Results (Rigid Rotor Blades)

- FM and C_Q can now within experimental error using engineering grids

	2007 SOA	2012 OVERFLOW	Improvement
FM	2.41%	0.22%	91%
C_Q	1.16%	0.17%	85%

- **Near-body accuracy is important, off-body accuracy not so important**
 - ❖ Combination of blade tip resolution/algorithm accuracy
 - 3rd-order convective differencing did poorly
 - 5th-order convective spatial differencing
 - ❖ DES length-scale crucial
 - Especially for lower collectives or resolved vortices
 - ❖ No ad-hoc methods are needed



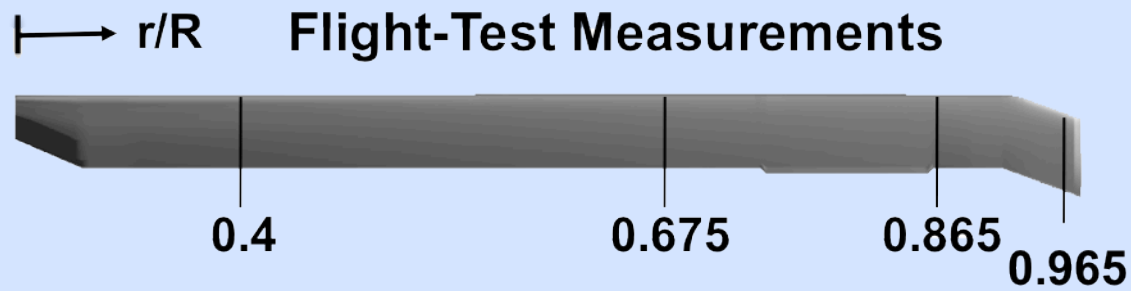
Summary of TRAM AMR Results (Rigid Rotor Blades)

- RANS length-scale can diffuse rotor wakes, even for non-BVI cases
 - ❖ Recall half of the rotor wake disappeared with AMR2
- AMR is needed to accurately predict vortex core size and growth rate
- Turbulent worms formed with AMR due to vortex stretching (typical of LES)
- DES is the near-term future of rotorcraft CFD
- LES is still limited to low Reynolds Numbers – for now!
- **Let's now look at the UH-60 flexible blade rotor in hover and forward flight**

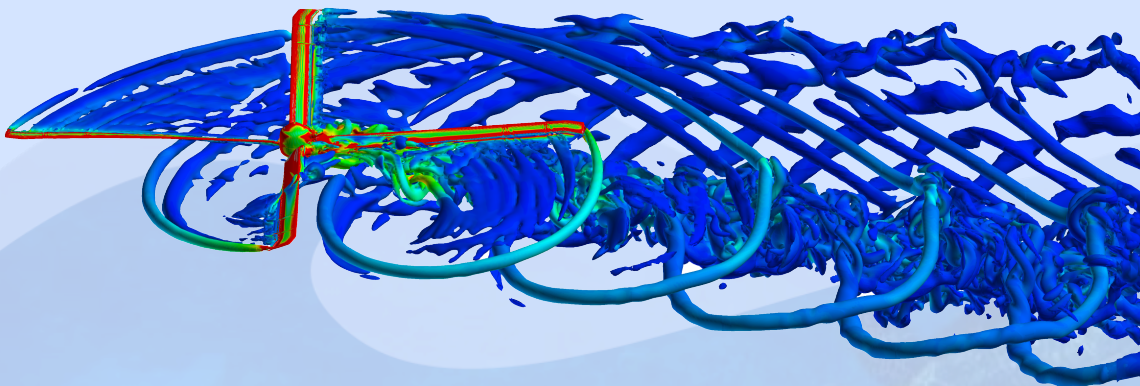


UH-60A in Forward Flight

Flexible Rotor: $M_\infty=0.236$, $M_{tip}=0.64$, $\mu=0.37$

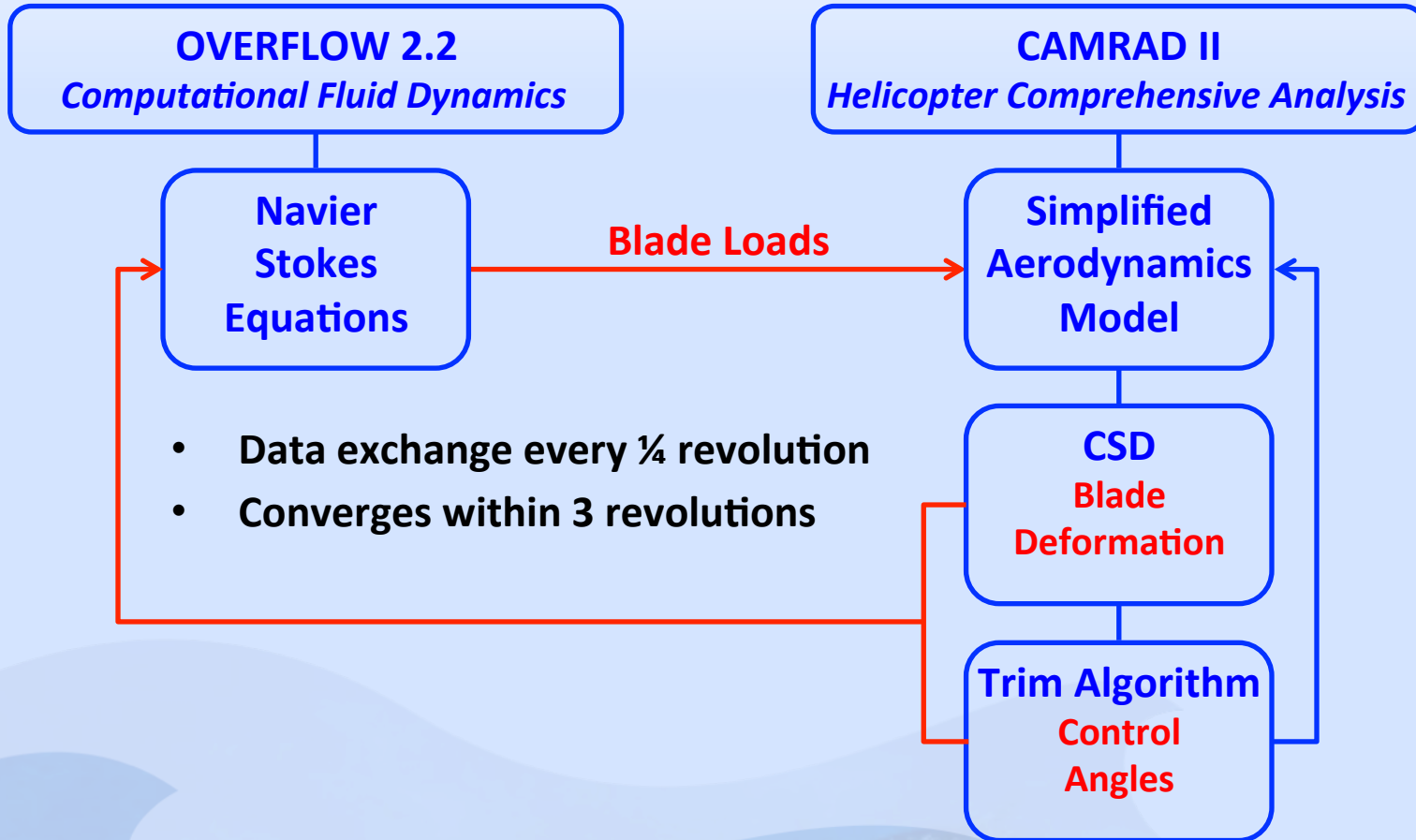


Flight Parameters: C8534	
M_∞	0.236
M_{tip}	0.64
$\mu=M_\infty/M_{tip}$	0.37
Shaft Angle	-7.31°
Sideslip Angle	1.28°
$Re_{tip/inch}$	3.3×10^5





Loose Coupling of CFD and Helicopter Comprehensive Codes



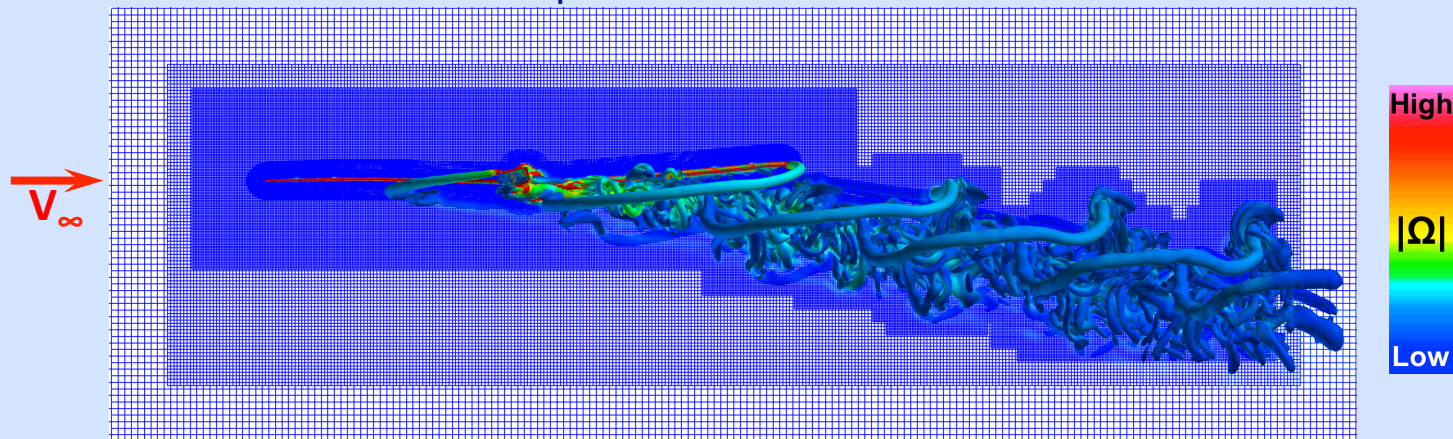


UH-60A in Forward Flight

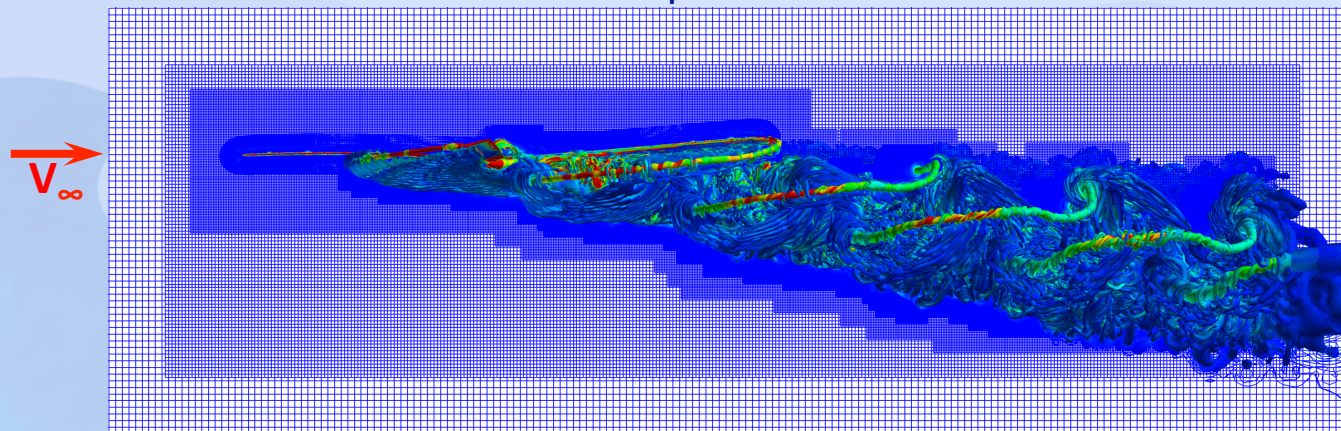
Flexible Rotor: $M_\infty=0.236$, $M_{tip}=0.64$, $\mu=0.37$

- AMR0 efficiently captures wake without grid refinement
 - ❖ 61 million grid points with uniform 10% c_{tip} grid
- AMR2 allows for efficient/automatic grid refinement

AMR0: $\Delta=10\%$ c_{tip} , 960 grids, 61 million grid points



AMR2: $\Delta=10\%$, 5%, and 2.5% c_{tip} , 18,500 grids, 754 million grid points

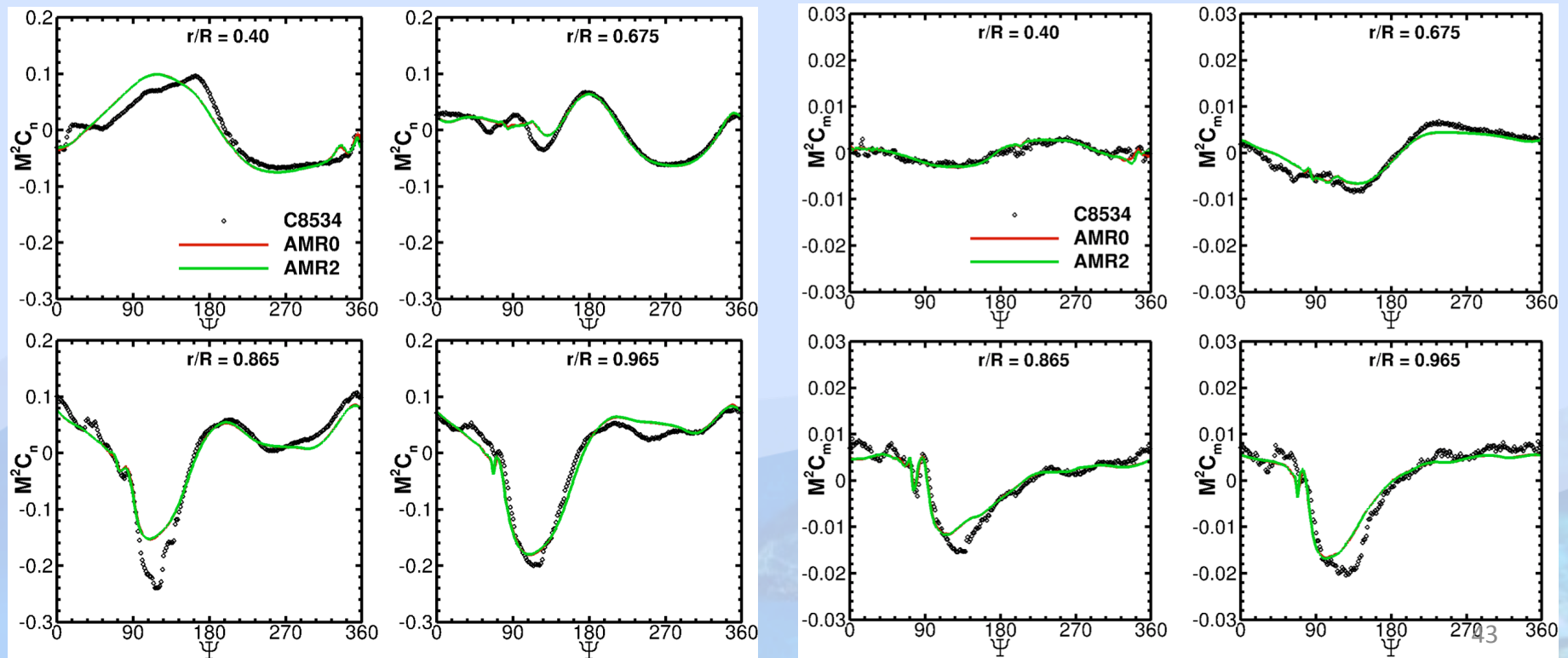




UH-60A in Forward Flight

Flexible Rotor: $M_\infty=0.236$, $M_{tip}=0.64$, $\mu=0.37$

- Normal force and pitching moment coefficients in good agreement with flight-test data
 - ❖ RMS error for integrated blade loads over one revolution
 - Normal force: 2.1%
 - Pitching moment: 2.5%
 - ❖ No difference in AMR0 and AMR2 for this case (no BVI)



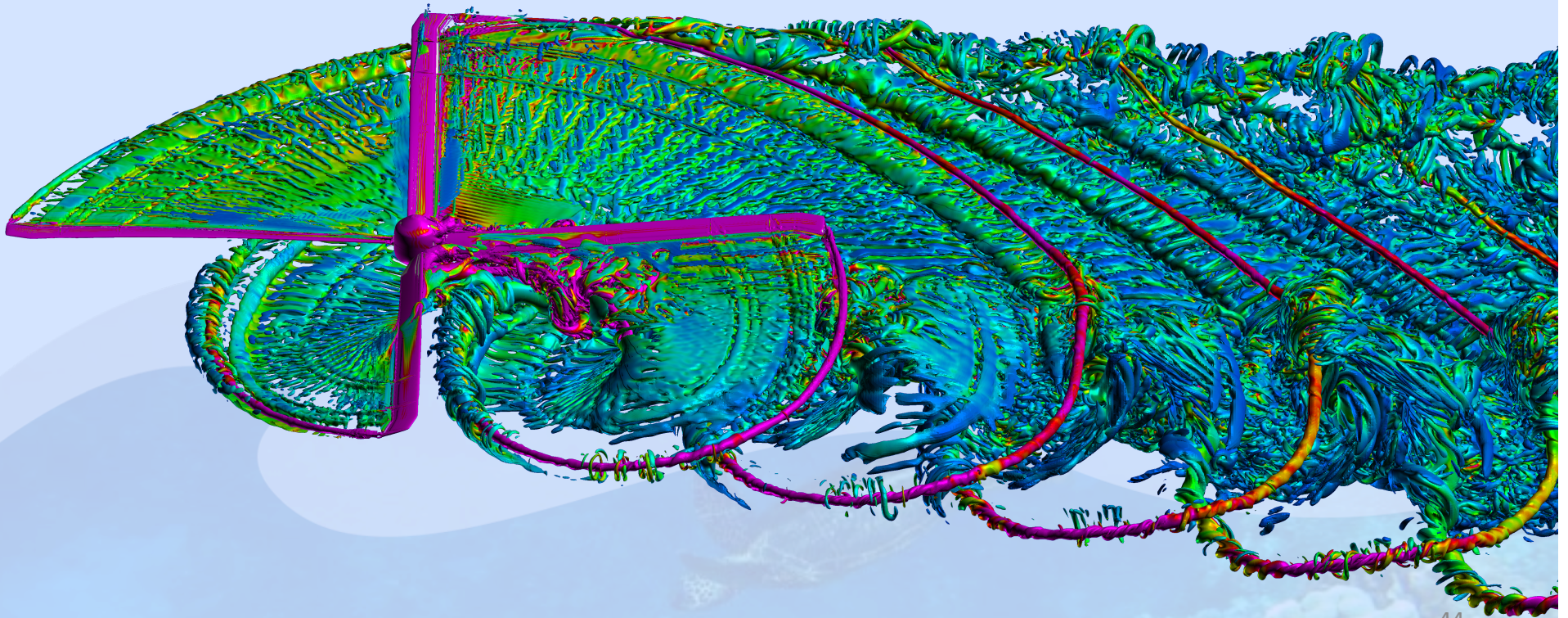


UH-60A in Forward Flight - AMR2

Flexible Rotor: $M_\infty=0.236$, $M_{tip}=0.64$, $\mu=0.37$

- All vortices captured, including the trim tab
- Radial lines of vorticity in wake shear layer
- Hub/blade interaction due to separation
- CFD/CSD/Trim loose coupling converges in 3 revolutions

Case	Grid Points (millions)	No. Cores	hr/rev
AMR0	61	1,536	5.4
AMR2	754	3,072	23.8



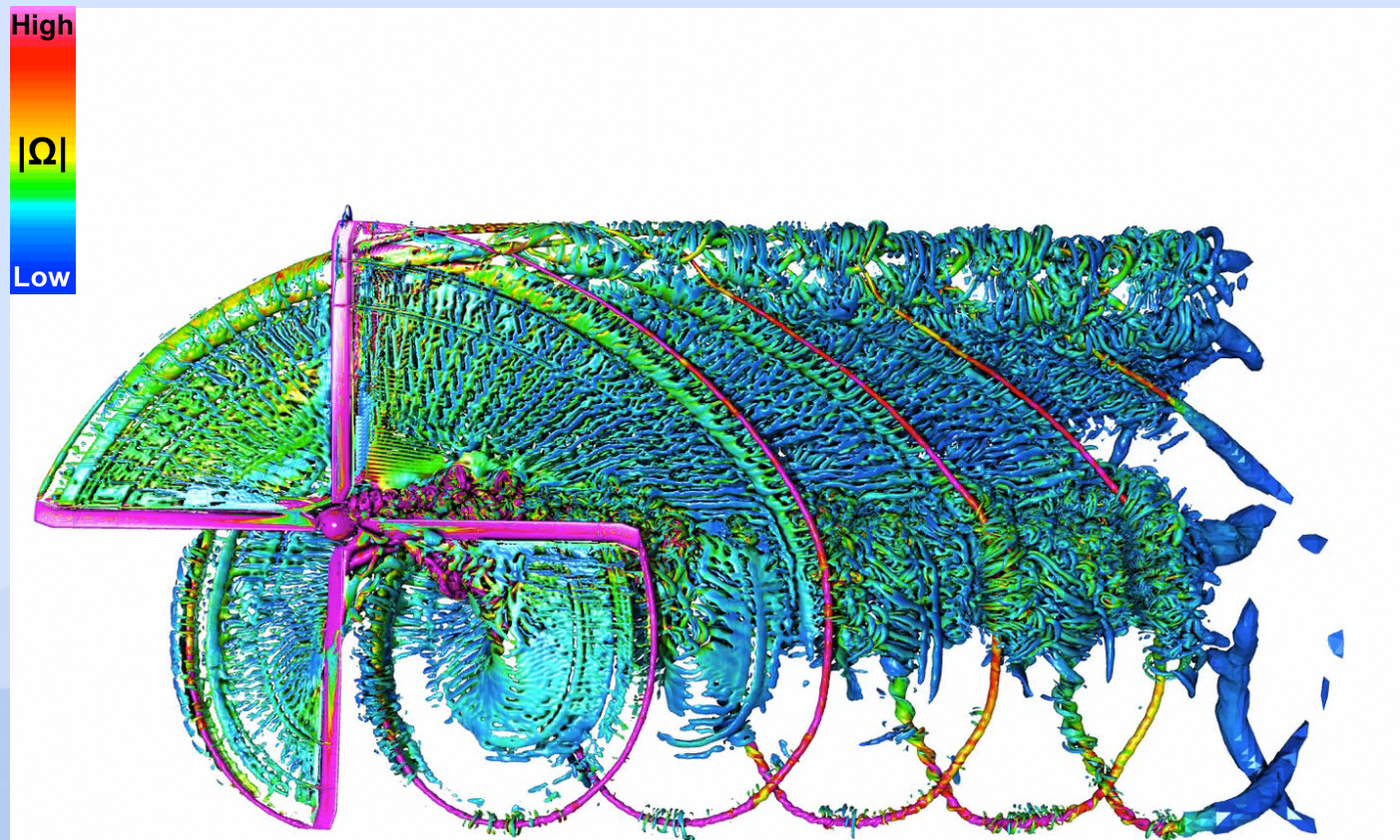


UH-60A in Forward Flight - AMR2

Flexible Rotor: $M_\infty=0.236$, $M_{tip}=0.64$, $\mu=0.37$

Visualization by Tim Sandstrom

q-criterion with shadows and ambient occlusion
provides greater 3D depth and shape cues

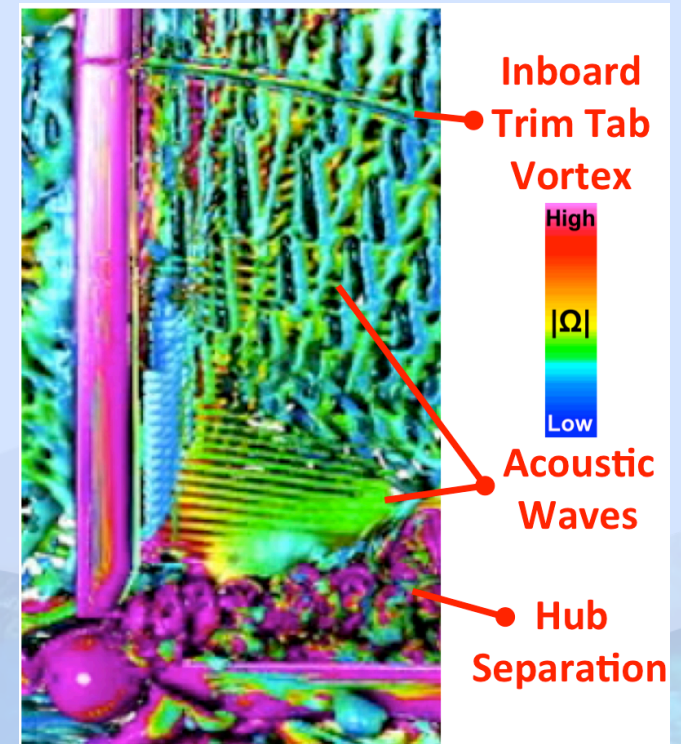
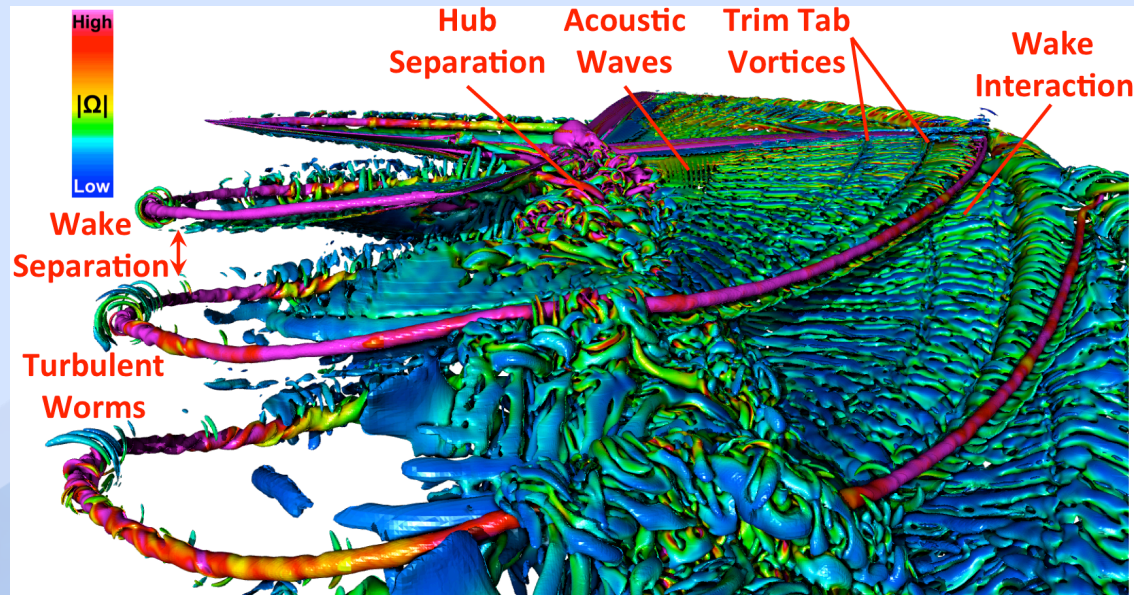




UH-60A in Forward Flight - AMR2

Flexible Rotor: $M_\infty=0.236$, $M_{tip}=0.64$, $\mu=0.37$

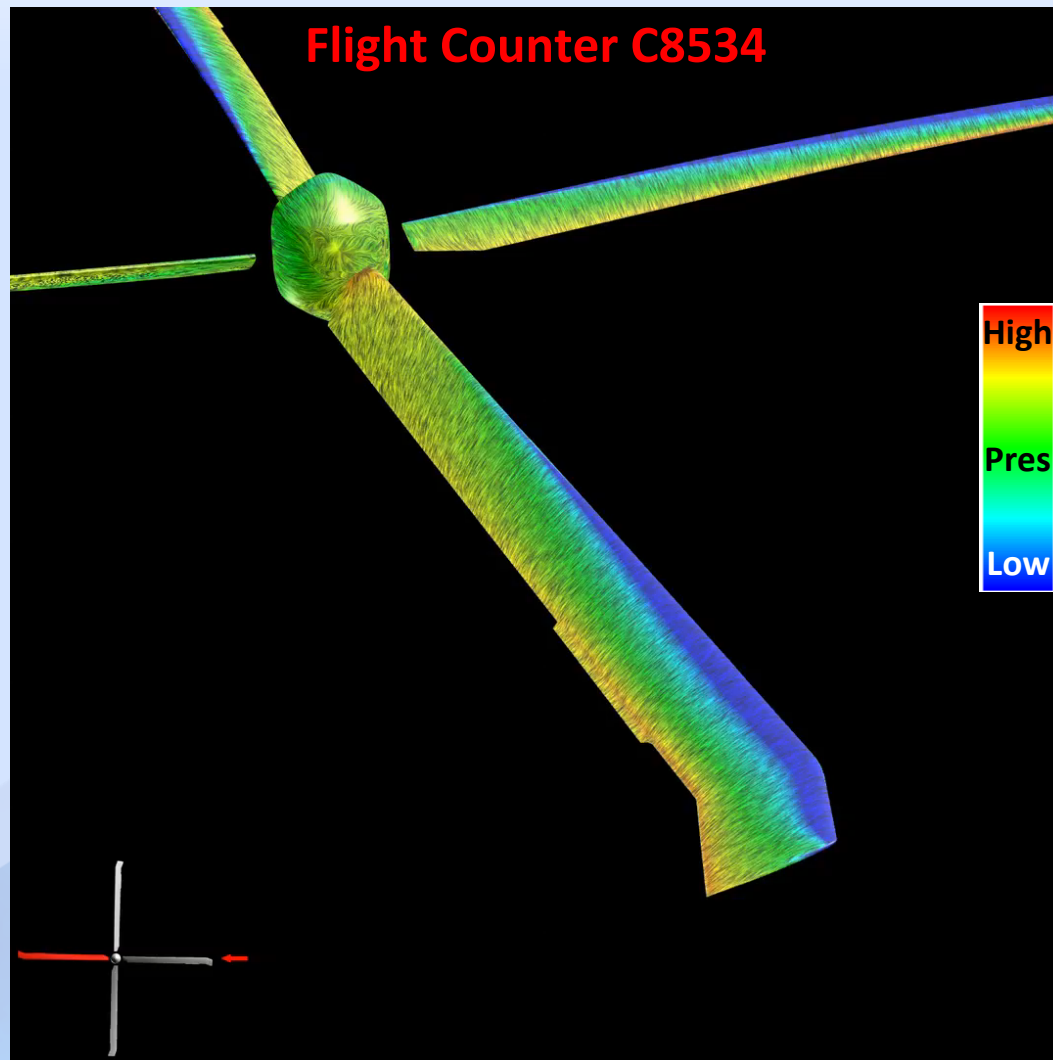
- Note few worms around vortices due to little interaction between vortices and wake shear layers
- Note acoustic waves
 - ❖ Due to hub separation brushing along the underside of the rotor blade





UH-60A in Forward Flight - AMR2

Time-Dependent Surface Flow Texture Mapping Colored by Pressure



- Shock appears as the blade advances
- Inboard separation as the blade retreats
- 3 ft vertical tip displacement



Summary of UH-60 Results

- High-order differencing and AMR demonstrated on flexible UH-60 rotor
- Benefits of AMR
 - ❖ Efficiently capture rotor wakes without apriori knowledge of the wake position
 - ❖ Resolve rotor wake in greater detail
- Computations were validated with experimental data
 - ❖ Forward flight normal force & pitching moment ~ 2% (2007 SOA ~ 4%)
- Turbulent worms also present with the UH-60 rotor

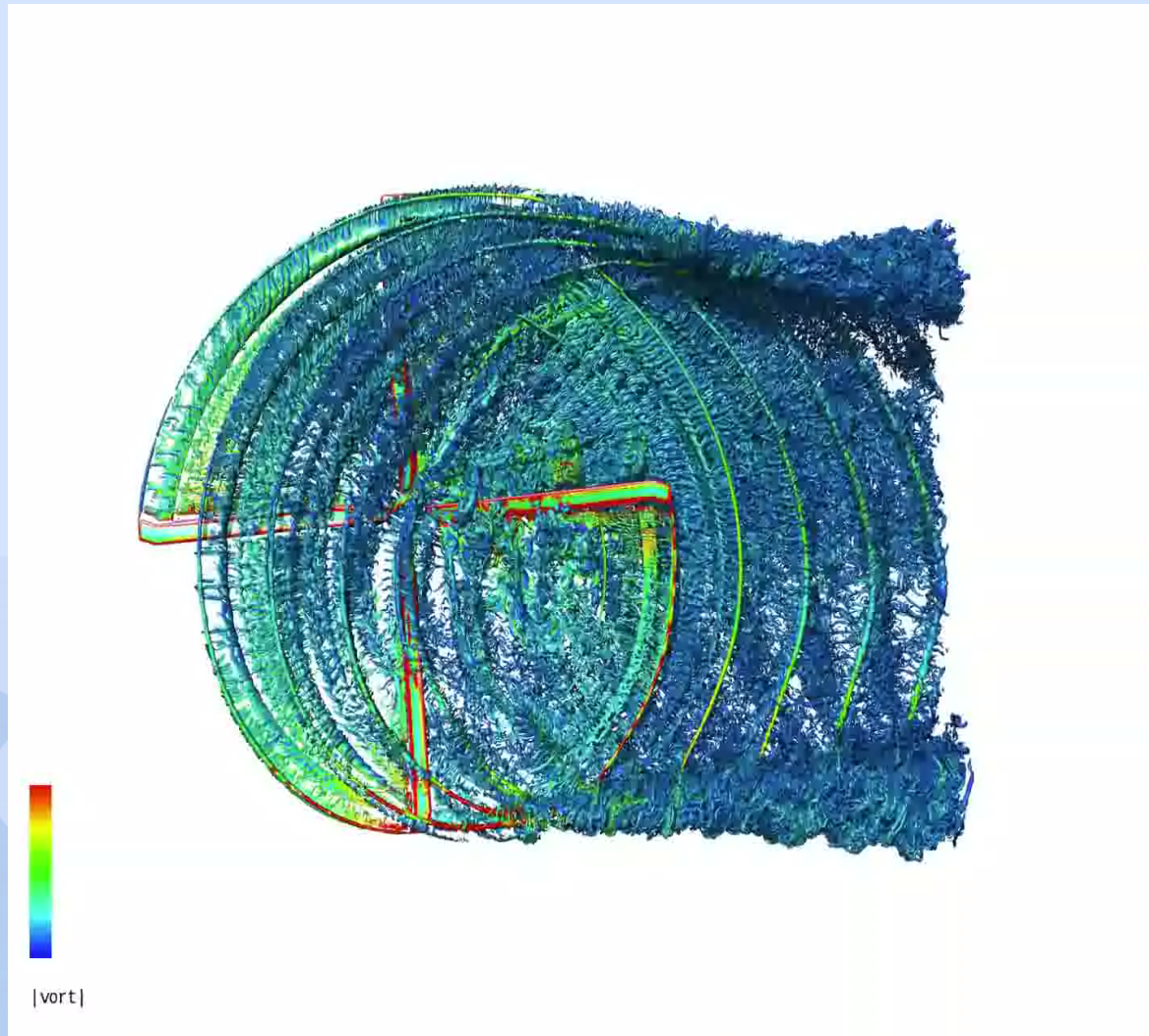


Time Dependent CFD Flow Visualization

$M_{tip}=0.65$, $\mu=0.15$, $\alpha=2.538$, $Re=7.3$ million

- Adaptive Mesh Refinement (AMR2): 12,400 grids, 725 million grid points
- Note many worms due to greater interaction between vortices and wake shear layers

Computations by Jasim Ahmad





State of the Art

- There have been significant improvement in CFD accuracy
- These improvements have **challenged** current experimental measurement technology
- CFD validation with experiment continues to be an important pacing item
- **Many of the legacy experiments are inadequate for modern CFD Codes**

**National Full-Scale Aerodynamics
Complex (NFAC) at NASA Ames**



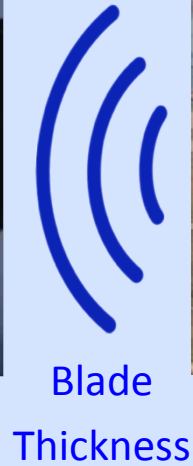
**Rotor Test Complex
(RTC) at NASA Langley**





Aeroacoustics

- Spanwise loads and shock waves transmit sound down
- Blade Thickness transmits sound ahead
- Rotor wakes create broadband noise
- The tail Rotor and other vehicle components create noise





Different Computational Aeroacoustics (CAA) Approaches

- Kirchhoff Integral
- Lighthill's analogy
- Ffowcs-Williams and Hawking (FW-H)
- Each of these methods have limitations
 - ❖ Linearized equations
 - ❖ Constraints on surface locations and flow conditions
 - ❖ **But all are based on the Navier-Stokes equations**
- **Can CAA accurately predict sound levels from first principals, i.e., directly from Navier-Stokes CFD?**

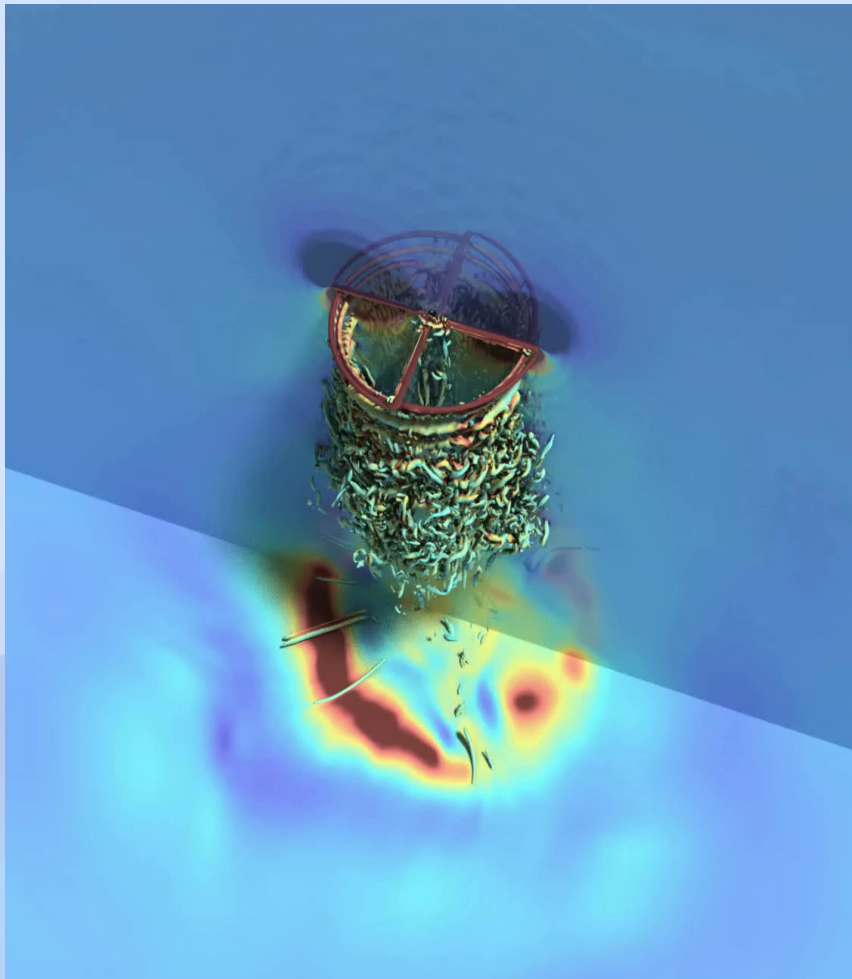




Navier-Stokes Pressure Field for a Hovering Rotor 20 ft above the NFAC floor

Rotor Radius=5ft, 80x120ft Test Section, $M_{\text{tip}}=0.63$, $\theta=12^\circ$, $Re=1.53$ million

Acoustic Pressure Waves on a Transparent Vertical Plane



- Sound is transmitted by weak pressure waves
 - ❖ $0.999 \leq P/P_\infty \leq 1.004$
- How can we visualize the flow to highlight the acoustic waves?

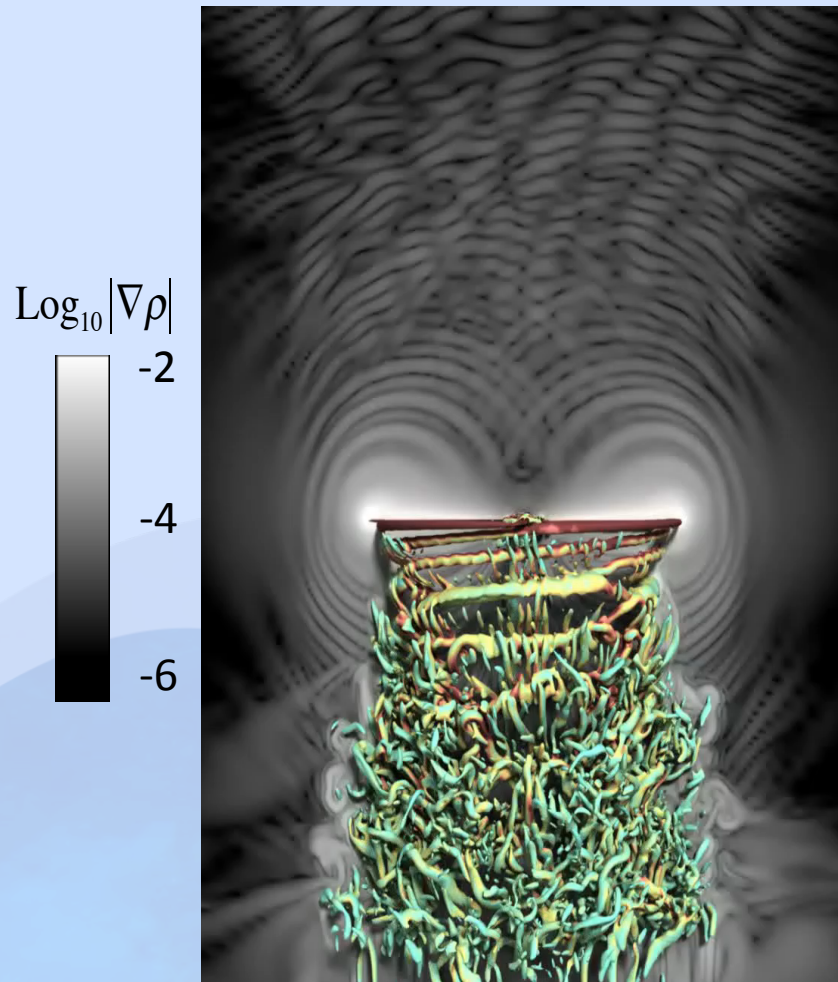


Navier-Stokes Acoustics for a Hovering Rotor 20ft Above the NFAC Floor

Rotor Radius=5ft, 80x120ft Test Section

$M_{tip}=0.63$, $\theta=12^\circ$, $Re=1.53$ million

Vertical Plane



- These acoustic waves are rendered by a numerical schlieren technique
- A vertical plane shows acoustic waves caused primarily by the pressure distribution along the rotor span
- An interference pattern forms above the rotor
- The waves merge farther from the rotor
- The rotor hub occasionally emits acoustic waves

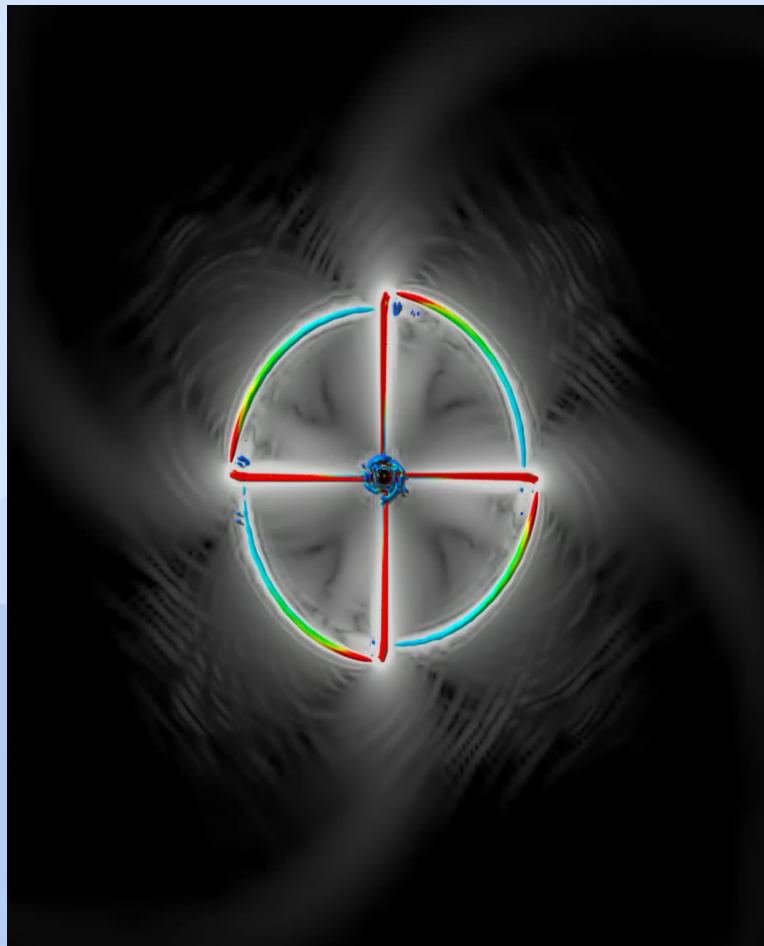


Navier-Stokes Acoustics for a Hovering Rotor 20ft Above the NFAC Floor

Rotor Radius=5ft, 80x120ft Test Section

$M_{tip}=0.63$, $\theta=12^\circ$, $Re=1.53$ million

Horizontal Plane



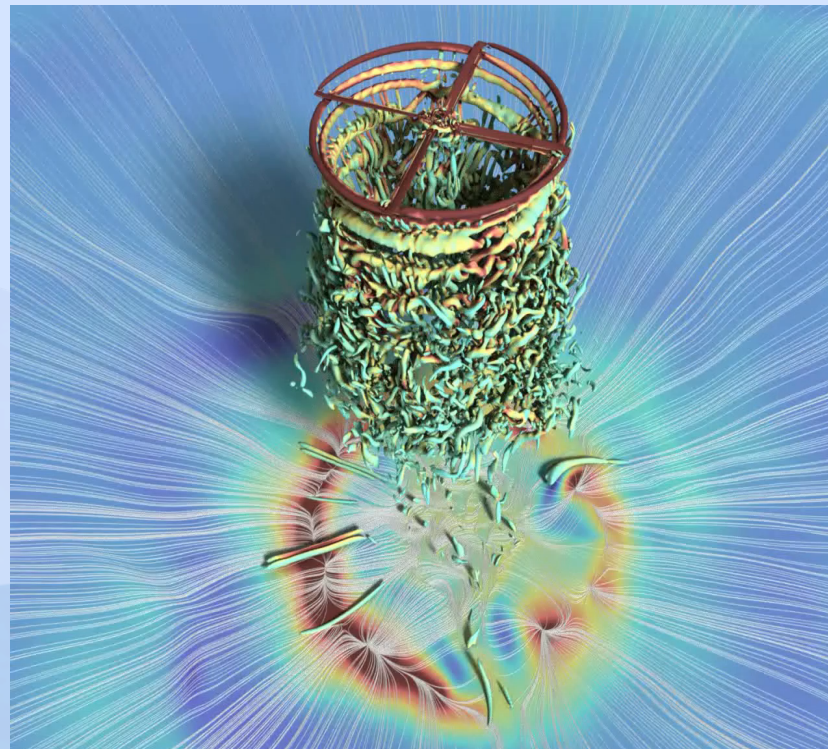
- These acoustic waves are rendered by a numerical schlieren technique
- The blade tips radiate waves outward
- The acoustic waves are due to the blade thickness displacing the air
- The blade tip waves merge to form spiral arms



Conclusions

- The decades-old problem of predicting hover performance within experimental error has been solved (from 2% to 0.2% error)
- Greatly improved vortex wake resolution and quantitative properties, including the CFD prediction of turbulent worms
- Many legacy experiments lack the precision to validate modern CFD codes
- Clusters can provide industry with accurate FM on baseline grids
- Supercomputing resources are necessary for detailed rotorcraft wakes

Rotor 20ft Above NFAC Floor
Time-Dependent Surface Flow



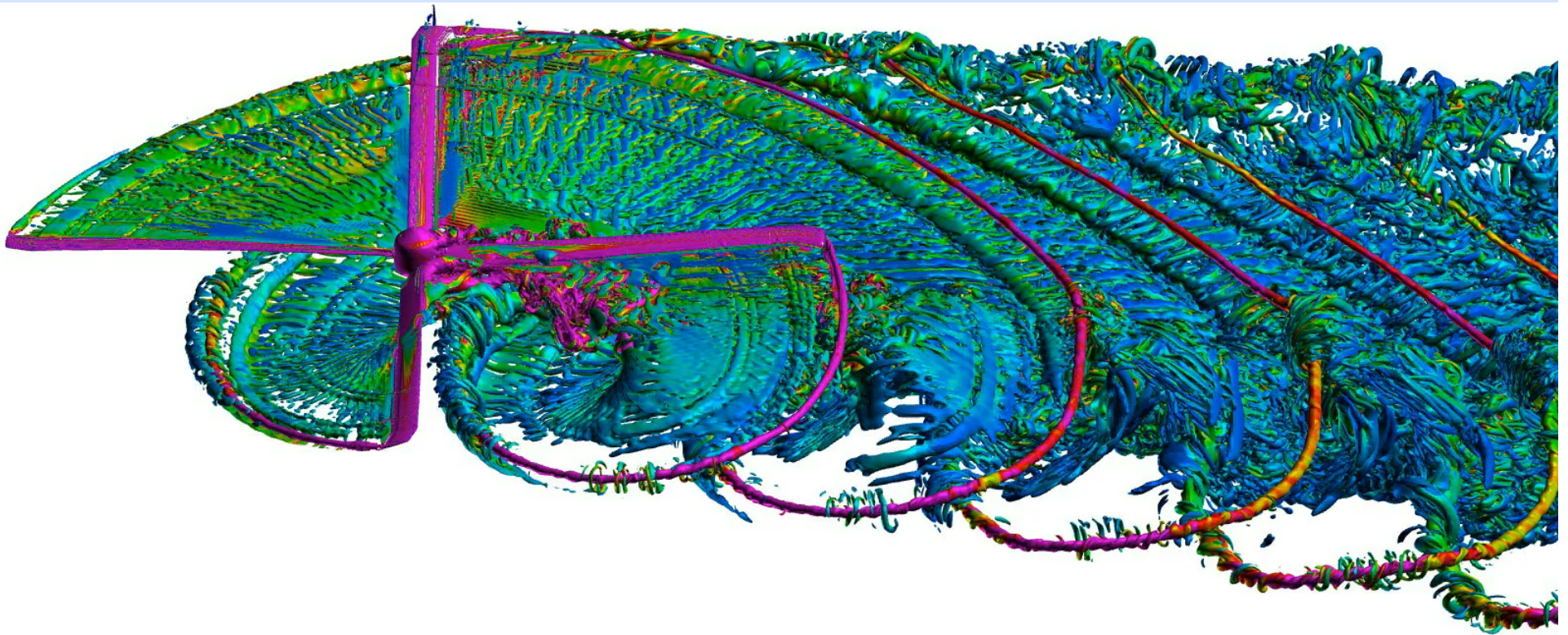


Future Work

- High-order temporal accuracy
- Improved hover convergence
- Near-body grid adaption
 - ❖ Dynamic stall
 - ❖ Need improvement in structural model?
- Adaptive flap control
 - ❖ Improve performance, reduce noise and vibration
- Acoustics?



**Thank You
Any Question?**





Extra Slides

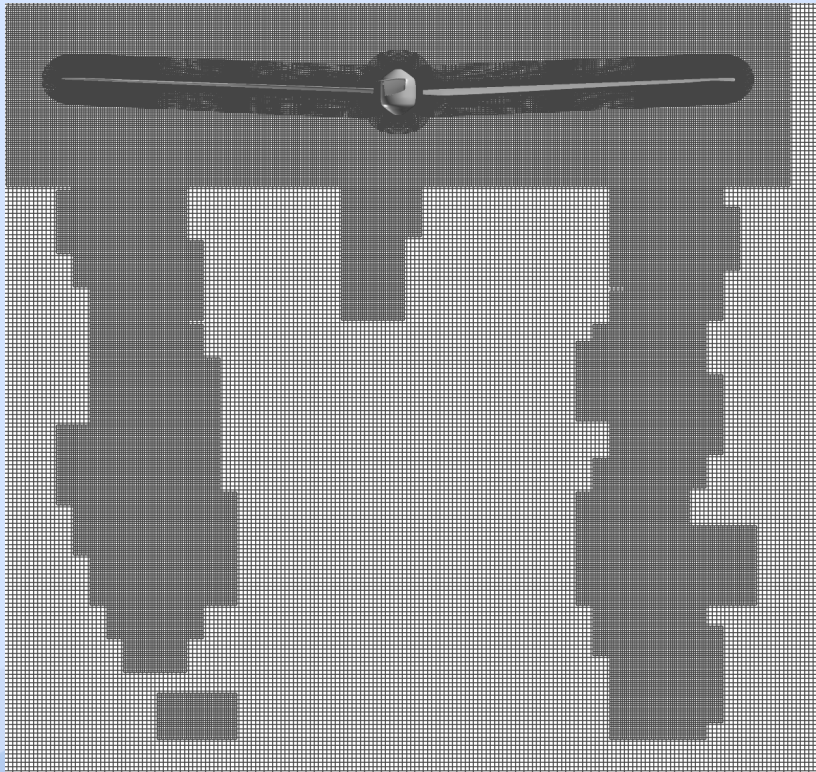




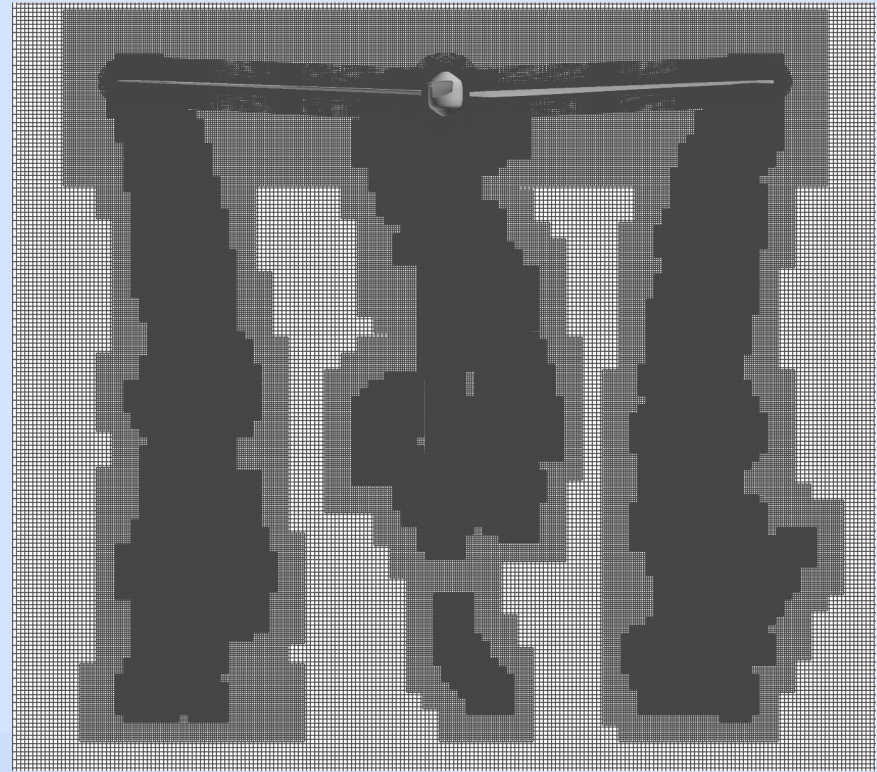
UH-60 in Hover

$$M_{\text{tip}}=0.628, C_T/\sigma=0.102, \sigma=0.825$$

AMR0: $\Delta=10\%$ c_{tip}
1,800 grids, 78 million grid points



AMR1: $\Delta=10\%$ and 5% c_{tip}
7,700 grids, 302 million grid points



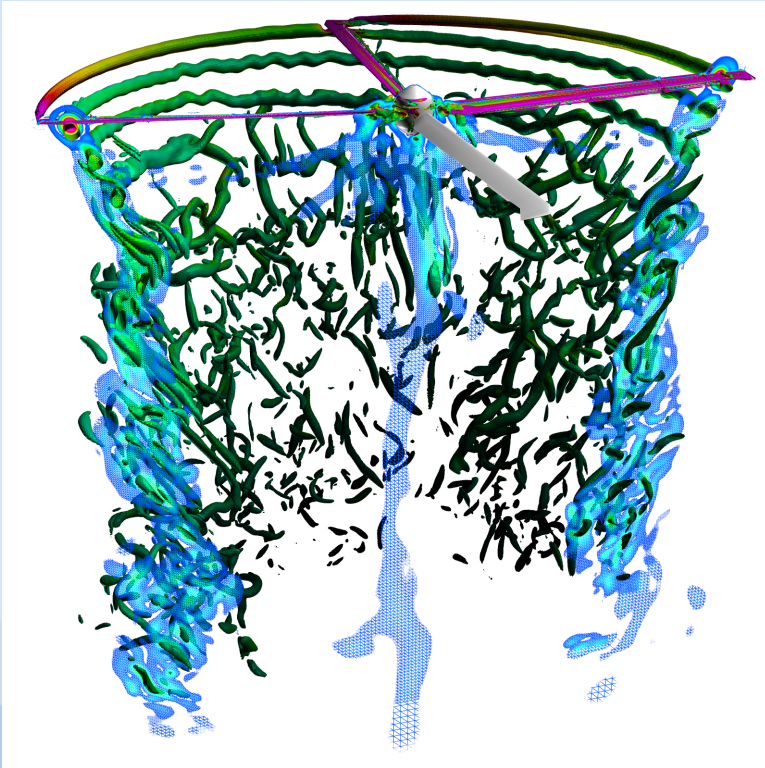


UH-60 in Hover

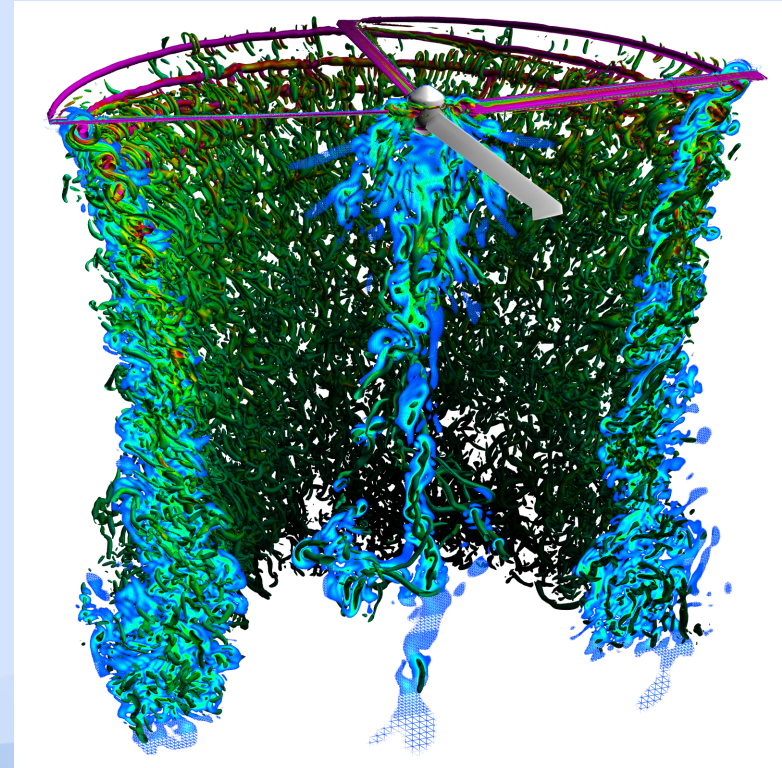
Vortical Worms Progression with Grid Resolution

$$M_{tip}=0.628, C_T/\sigma=0.102, \sigma=0.825$$

AMR0: $\Delta=10\%$ c_{tip}



AMR1: $\Delta=10\%$ and 5% c_{tip}

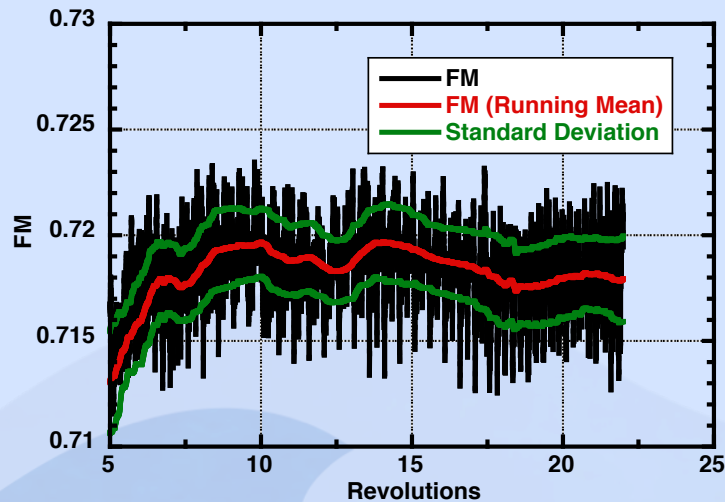




UH-60 in Hover

$$M_{\text{tip}}=0.628, C_T/\sigma=0.102, \sigma=0.825$$

- UTRC WT FM = 0.734
- Corrected FM = 0.72 (estimate)
 - ❖ Residual thrust due to imperfect/worn transfer coupling (Peter Lorber, principal investigator)
- Computational precision tends to be higher than experimental measurement precision



Case	FM	Error	Grid Points (millions)	Cores	hr/rev
AMR0	0.719	0.1%	78	1536	5.8
AMR1	0.718	0.3%	302	4608	10.1



Comparison of AMR2 Wake with Uniform Grid Spacing

TRAM Hover: $M_{tip}=0.625$, $\theta=14^\circ$, $Re=2.1$ million, DES

No significant difference between AMR2 and uniform mesh vorticity contours

